energies

MDPI

Review

Functionalization Strategies of MXene Architectures for Electrochemical Energy Storage Applications

Shude Liu [1,2,*], Huilin Zhang [1], Jieming Chen [1], Xue Peng [1], Yafei Chai [1], Xian Shao [1], Yi He [1], Xiaoqiang Wang [1] and Bin Ding [1,3,*]

[1] Engineering Research Center of Technical Textile, Ministry of Education, College of Textiles, Donghua University, Shanghai 201620, China; 2230287@mail.dhu.edu.cn (H.Z.); 2230280@mail.dhu.edu.cn (J.C.); 2230315@mail.dhu.edu.cn (X.P.); 2240261@mail.dhu.edu.cn (Y.C.); 2240185@mail.dhu.edu.cn (X.S.); 2240229@mail.dhu.edu.cn (Y.H.); 2240011@mail.dhu.edu.cn (X.W.)
[2] Department of Materials Process Engineering, Graduate School of Engineering, Nagoya University, Nagoya 464-8603, Japan
[3] Innovation Center for Textile Science and Technology, College of Textiles, Donghua University, Shanghai 201620, China
* Correspondence: sdliu@dhu.edu.cn (S.L.); binding@dhu.edu.cn (B.D.)

Abstract: MXene, an emerging class of two-dimensional materials, has garnered significant attention in electrochemical energy storage applications due to its high specific surface area, tunable surface functional groups, excellent electrical conductivity, and mechanical stability. However, their practical application in energy storage devices remains challenged by issues such as the stacking of their layered structure, surface degradation, and limited ion diffusion properties. Functionalization has emerged as a key strategy to enhance the performance of MXene materials. By modulating surface functional groups, doping with various elements, and integrating with other materials, researchers have significantly improved the electrical conductivity, chemical stability, ion transport properties, and mechanical strength of MXenes. This review provides a comprehensive overview of MXene materials, categorizing them and highlighting their advantages in electrochemical energy storage applications. It also examines recent advancements in MXene preparation and optimized synthesis strategies. In-depth discussions are presented on the functionalization of MXenes and their applications in energy storage devices, including supercapacitors, lithium-ion batteries, and sodium-ion batteries. Finally, the review concludes with a summary of the practical applications of MXenes and explores future research directions, aiming to guide further developments in the energy storage field.

Keywords: MXene; functionalization strategies; electrochemical energy storage; structural design

check for updates

Received: 16 February 2025
Revised: 26 February 2025
Accepted: 27 February 2025
Published: 2 March 2025

Citation: Liu, S.; Zhang, H.; Chen, J.; Peng, X.; Chai, Y.; Shao, X.; He, Y.; Wang, X.; Ding, B. Functionalization Strategies of MXene Architectures for Electrochemical Energy Storage Applications. *Energies* **2025**, *18*, 1223. https://doi.org/10.3390/en18051223

Copyright: © 2025 by the authors. Licensee MDPI, Basel, Switzerland. This article is an open access article distributed under the terms and conditions of the Creative Commons Attribution (CC BY) license (https://creativecommons.org/licenses/by/4.0/).

1. Introduction

Two-dimensional (2D) materials are substances consisting of single or few atomic layers, exhibiting remarkable physical, chemical, and mechanical properties [1]. These distinctive characteristics have garnered significant attention in various fields, including electronics, energy storage and conversion, catalysis, sensors, and flexible electronics [2]. Prominent examples of 2D materials include graphene, transition metal dichalcogenides (TMDs), and black phosphorus (P), among others [3,4]. Among them, MXene, as an emergent 2D material, has garnered an amount of research attention due to its excellent multifunctional attributes [5,6]. MXene materials could be described as transition metal carbides, nitrides, and their compounds, featuring a unique 2D layered structure with alternating

layers of transition metal atoms and carbon or nitrogen atoms [7,8]. This configuration bestows MXene materials with an extremely high specific surface area, superior electrical conductivity, favorable mechanical strength, and remarkable electrochemical activity, enabling them to exhibit tremendous application potential in the field of electrochemical energy storage [9–11]. Nevertheless, the performance of MXene in practical electrochemical energy storage devices is still subject to certain limitations [12]. Firstly, the layered structure of MXene materials is prone to stacking and aggregating during the charging and discharging processes, resulting in a reduction in the available specific surface area [13]. Secondly, the surface of MXene materials often contains functional groups, such as oxides and fluorides, which might undergo unstable reactions upon contact with the electrolyte, leading to surface degradation during long-term usage and subsequently influencing cycling stability [14,15]. Finally, the ion diffusion rate of MXene materials is constrained by the interlayer spacing and surface morphology, which may cause a deterioration in electrochemical performance under high-rate charging and discharging conditions [16,17]. Therefore, it is imperative to overcome these challenges to further enhance the electrochemical performance of MXene materials and facilitate their application in electrochemical energy storage devices.

In recent years, the functionalization of MXene materials has offered great opportunities for their applications [18,19]. The electrical, chemical, and mechanical properties of MXene materials have been effectively enhanced by introducing surface chemical state regulating, foreign element doping, and compound fabricating. In detail, the self-stacking phenomenon can be effectively mitigated by the modulation of surface functional groups, which could also enhance the surface activity of MXene materials [20,21]. Element doping, such as nitrogen, sulfur, and P or compounds involving carbon-based materials and transition metal oxides (TMOs), could not only boost the electronic conductivity of MXene materials but also improve their interface stability and ionic transport ability [22–24]. In addition, the electrochemical performance can be further improved by adjusting the interlayer spacing of MXene materials or constructing a heterojunction structure. By effectively controlling the "space charge effect" at the interface, including the interface electric field and the space charge region, the energy storage advantages at the surface, bulk phase, and interface can be fully optimized [25,26]. These research findings indicate that the functionalization of MXene materials has garnered increasing attention [27]. However, most existing research reviews focus on the preparation methods or performance in the specific applications of MXene materials but lack the systematical investigation of the functionalization modification methods of MXene materials for enhanced performance in electrochemical energy storage applications [28–30]. For example, Hussain et al. [31] summarized the applications and challenges of non-titanium MXenes in energy storage and conversion; however, their discussion primarily focused on the applications of non-titanium MXenes across various energy storage devices and energy conversion systems, without addressing the specific challenges these materials face in these areas or proposing optimization strategies. Similarly, while Patil et al. [32] provided valuable insights into the synthesis and application of MXenes for micro-supercapacitors and micro-batteries, their review lacked an in-depth analysis of the functionalization strategies necessary to optimize MXene architectures specifically for enhancing electrochemical energy storage performance. Simultaneously, as new modification methods and technologies emerge, traditional reviews often fail to cover the latest research advancements comprehensively [33].

This review aims to address the existing gap by systematically summarizing recent advancements in the functionalization of MXene materials for electrochemical energy storage, providing a comprehensive analysis of the improvements in their performance. The review begins by introducing the structure and advantages of MXene materials, with a

particular focus on their unique characteristics in the context of energy storage. The primary preparation methods of MXene materials will be summarized, along with their influence on the structural and surface chemical properties of MXenes. Next, the challenges faced by MXene materials in electrochemical energy storage, particularly in terms of stability and performance, will be discussed. The functionalization strategies of MXene materials will then be explored in detail, along with their applications in energy storage devices, such as supercapacitors, lithium-ion batteries, and SIBs. Furthermore, the review will address the challenges and prospects of MXene materials in electrochemical energy storage, presenting strategies for enhancing their widespread applications.

2. Fundamentals of MXene Materials

2.1. Composition and Structure of MXenes

MXenes are a class of 2D materials composed of transition metal carbides, nitrides, or carbonitrides, with the general formula $M_{n+1}X_nT_x$. Several common MXene structures are illustrated in Figure 1a. In this formula, M represents transition metal elements, such as Ti, V, Cr, Mo, etc.; X denotes C or N; and T_x refers to the surface functional groups and their quantities, such as -OH, -O, -F, as shown in Figure 1b [34]. MXenes are synthesized through selective etching of the A layer from the MAX phase, forming a 2D structure, as depicted in Figure 1c [35]. In the MAX phase, M and X atoms are covalently and ionically bonded to form a hexagonal crystal structure. The A layer alternates with the M-X layers, with weaker metallic bonds connecting the M atoms to the A layers [36]. Under appropriate conditions, selective etching removes the A layer, while retaining the M-X layers, resulting in a 2D structure composed of transition metals and carbon or nitrogen atoms.

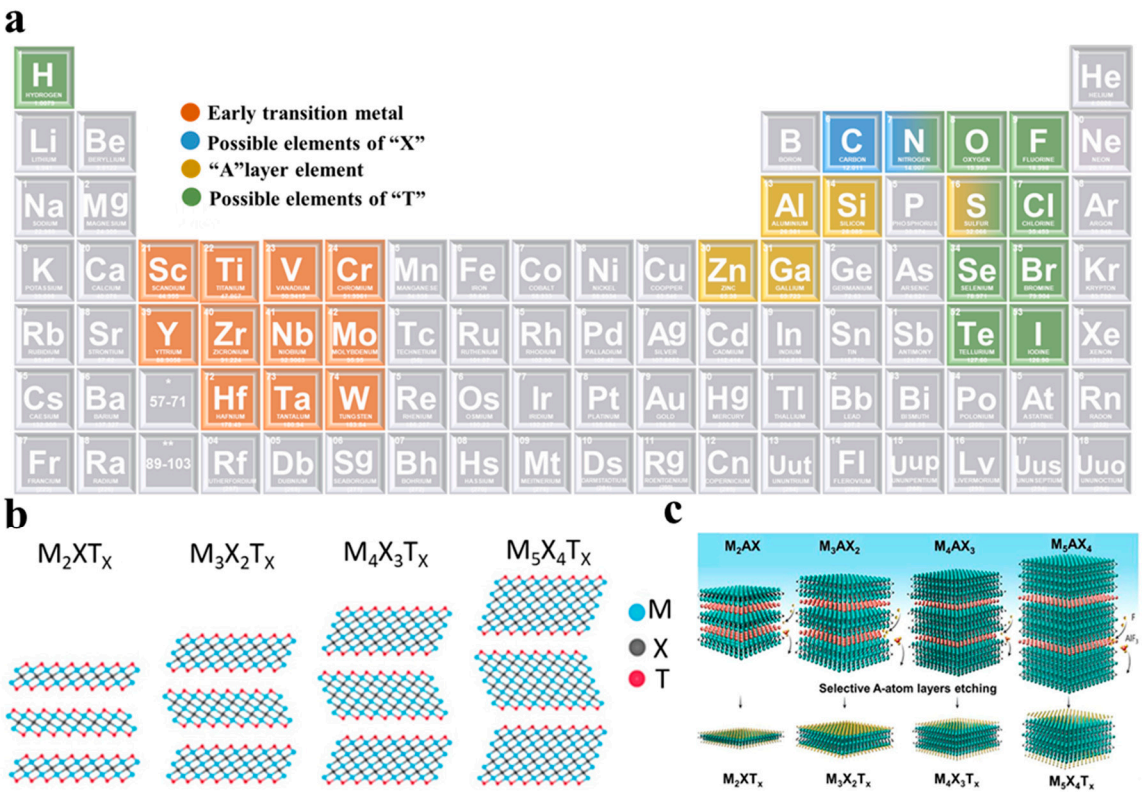


Figure 1. *Cont.*

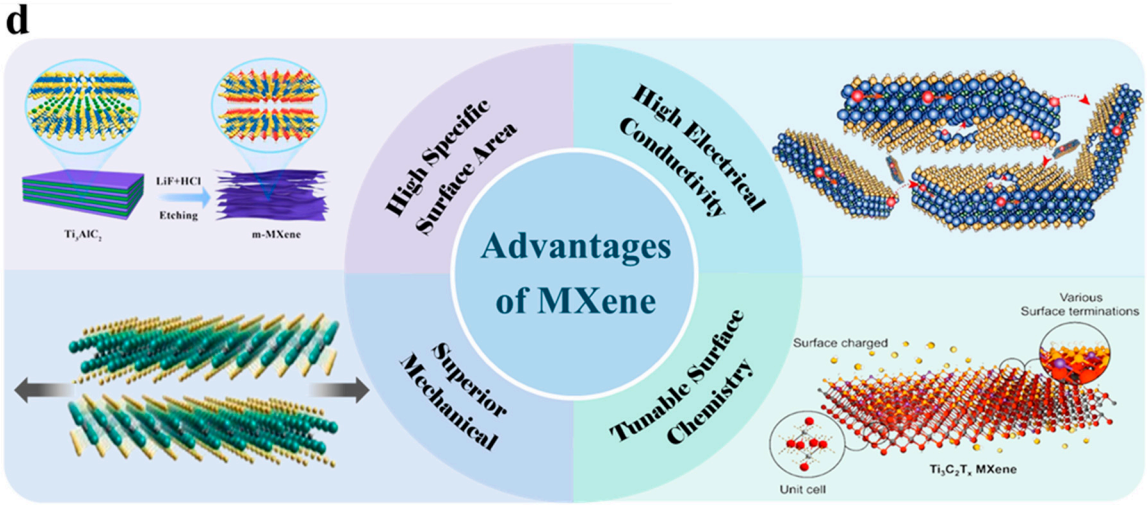


Figure 1. (**a**) The periodic table showing the elements that have been experimentally employed in the synthesis of MXenes, serving as the "A" layer, which has been successfully etched. (**b**) Structural representations of MXenes with varying atomic layers, where n ranges from 1 to 4. Reproduced with permission [34]. Copyright 2024, Wiley-VCH. (**c**) The MAX phases and their corresponding MXene structures. Reproduced with permission [35]. Copyright 2022, Science Press. (**d**) A summary of the key advantages of MXene materials.

2.2. Merits of MXene

The structure of MXene materials presents several distinct advantages (Figure 1d). Specifically, the layered architecture of MXene, akin to graphene and TMDs, offers a large specific surface area, thereby providing abundant active sites for enhanced ion storage and electron conduction. Furthermore, the interlayer spacing in MXene can be precisely adjusted through surface functionalization or chemical etching, enabling its optimization for various electrochemical environments and improving its ion storage capacity. In addition, MXene demonstrates high electrical conductivity and robust mechanical properties, which contribute to its stability during rapid charge–discharge cycles. The material also features versatile surface chemistry, which can be tailored through functionalization to further enhance its electrochemical performance in diverse energy storage systems. Overall, the unique layered structure and tunable properties of MXene make it a promising candidate for advanced energy storage applications.

2.2.1. High Specific Surface Area

The distinctive layered architecture of MXenes provides an exceptionally high specific surface area, offering numerous reactive sites for ions. This characteristic not only significantly enhances the electrode–electrolyte interface, thereby improving charge storage efficiency and energy density, but also facilitates rapid ion transport, reducing diffusion distances and enabling high power density and fast charge–discharge capabilities. For instance, Wei et al. [37] employed a scalable, simple electrostatic self-assembly approach to construct an MXene/organic heterostructure, which effectively mitigated the solubility issue of PTCDA in organic liquid electrolytes. The large surface area of 2D MXene nanosheets, combined with electrostatic self-assembly, resulted in the PTCDA particles being encapsulated by the MXene nanosheets, minimizing direct interaction with the electrolyte and, thus, slowing the dissolution of PTCDA. This strategy notably improved the cycling performance of PTCDA-based organic batteries.

2.2.2. High Electrical Conductivity

MXenes exhibit exceptional electrical conductivity, with values ranging from 6000 to 8000 S cm^{-1}. This high conductivity can be attributed to two primary factors. Firstly, the d-orbital electrons of the transition metal M in MXenes contribute a high electron density near the Fermi level, resulting in an increased density of states at this energy level, which facilitates electron transport and significantly enhances conductivity [38,39]. Secondly, the weak van der Waals forces between MXene layers create interlayer spaces that allow for free electron migration within the layers, forming conductive pathways and improving electron mobility, thereby contributing to their outstanding electrical conductivity [40].

2.2.3. Superior Mechanical Properties

MXenes are characterized by strong M-N and M-C bonds, as well as a densely stacked layered structure, which ensures their mechanical stability [41]. Compared to the parent MAX phases, MXenes exhibit higher strength and durability, likely due to the removal of the A layer, which leads to an accumulation of electron density between the layers, enhancing the M-X bond strength [42]. For example, the robust M-C bonds in 2C MXenes impart a high elastic modulus and ideal strength under biaxial stress, further demonstrating that Mo_2C is an excellent elastic material with substantial strain resilience [43]. This stability allows MXenes to effectively withstand electrode degradation caused by volume changes during charge and discharge cycles, ensuring the long-term cycling stability of energy storage devices [44].

2.2.4. Tunable Surface Chemistry

MXenes also possess tunable surface chemistry, and modifying their surface functional groups allows for further adjustments to their electronic structure and electrochemical properties, thus meeting the diverse requirements of various energy storage applications. For example, Kamysbayev et al. [45] introduced a versatile strategy for modulating MXene surface functional groups through substitution and elimination reactions in molten inorganic salts. This approach successfully synthesized MXenes with a range of functional groups, including -O, -S, -Cl, -Se, -Br, and -Te, as well as MXenes with no surface functional groups. The resulting MXenes exhibited distinct structural and electronic properties. Studies demonstrated that surface functional groups can influence the atomic spacing in the MXene lattice, with Te_2-ligands in $Ti_{n+1}C_n$ (n = 1, 2) leading to significant planar lattice expansion (>18%) compared to TiC lattices [39]. Additionally, Nb_2C MXenes exhibited surface functional group-dependent superconductivity.

3. Synthesis Methods of MXenes

The preparation methods of MXene primarily include the fluorine-containing method, fluorine-free method, and molten salt method (Figure 2). The fluorine-containing method involves etching the Ti_3AlC_2 precursor with ammonium fluoride or hydrogen fluoride solution to selectively remove the aluminum layer, yielding MXene with high conductivity and a large specific surface area. However, this method poses safety concerns due to the corrosive nature of the fluorine-containing reagents. In contrast, the fluorine-free method utilizes reagents, such as ammonium chloride or sodium chloride, mitigating the safety risks associated with fluorinating agents, and has become an increasingly popular alternative. The molten salt method, on the other hand, involves heating the precursor with molten salts (e.g., sodium chloride or potassium chloride) at high temperatures to selectively etch away the aluminum layer. This approach allows for precise control over the reaction temperature and offers the advantage of optimizing the morphology and properties of the resulting MXene.

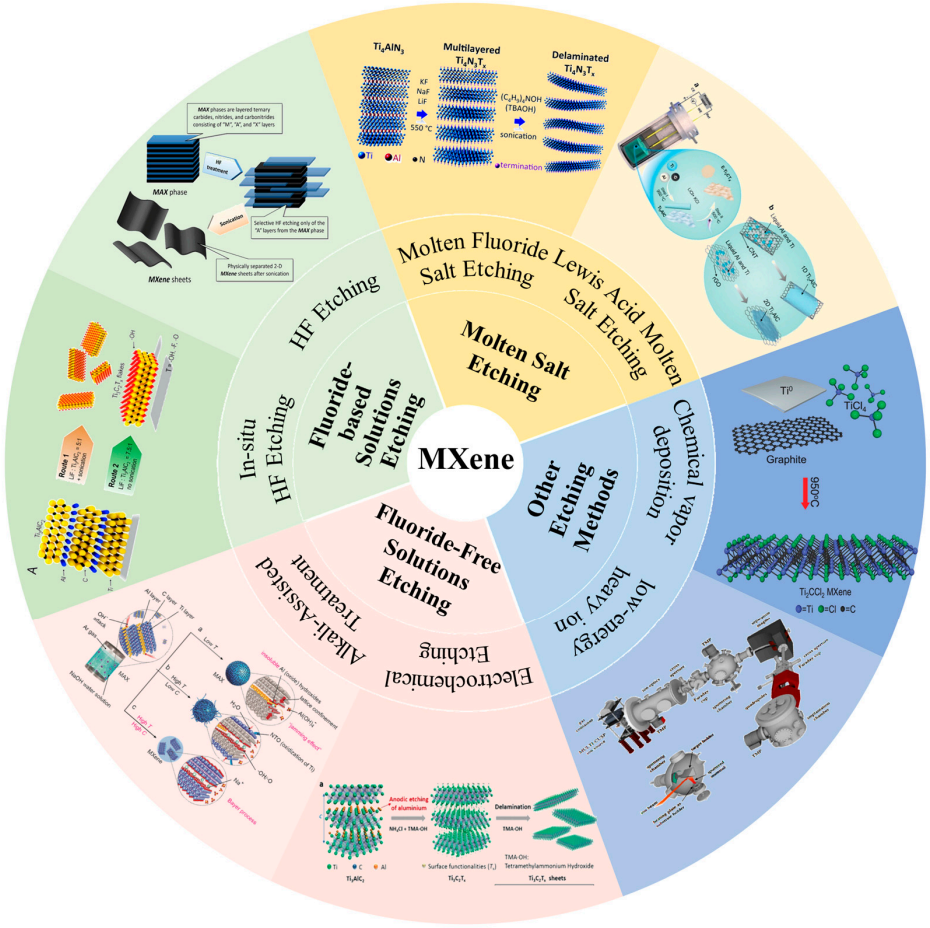


Figure 2. Various techniques for the synthesis of MXene materials.

3.1. Fluoride-Containing Solution Etching

3.1.1. HF Etching

Hydrofluoric acid (HF) etching is the earliest and most traditional method for the preparation of MXenes [46]. This technique involves the selective etching of the A-layer atoms from the MAX phase using an HF solution, resulting in multi-layered MXenes. The first synthesis of MXenes was achieved by etching the precursor Ti_3AlC_2 with HF. Gogotsi et al. [47] demonstrated that HF, through a simple substitution reaction, effectively extracts Al atoms from Ti_3AlC_2, simultaneously releasing H_2. During this process, both H_2O and HF molecules react with the resulting Ti_3C_2, forming $Ti_3C_2T_x$, where T represents surface terminations, such as -OH, -F, and -O, while simultaneously releasing additional H_2 [48]. According to first principles calculations, the etching process begins with HF intercalating into the edges of the MAX phase, gradually penetrating deeper as the reaction progresses. The formation of Ti-F bonds weakens the Al-Ti bond, resulting in an expansion of the interlayer spacing in the MXenes, which further facilitates HF intercalation and, ultimately, leads to the formation of AlF_3, successfully etching away the Al atomic layer. Importantly, the MXenes produced by this method retain their layered structure, as van der Waals forces and hydrogen bonding continue to exist between the layers [49]. This HF etching approach is effective for most Al-containing MAX phase materials, allowing the successful synthesis of a wide range of MXenes (e.g., Mo_3C_2, V_2C, and $Mo_2Ti_2C_3$), with the resulting MXenes exhibiting a high density of -F surface functional groups, significantly improving the yield. However, due to HF's highly corrosive nature, safety risks during the etching process are relatively high [50]. Additionally, improper concentration or etching time can lead to excessive defects or a reduction in the size of the synthesized MXenes.

3.1.2. In Situ HF Etching

To mitigate the corrosion and safety concerns associated with direct HF usage, researchers have developed milder and safer etching strategies. These methods involve using fluoride salts, such as LiF/HCl, NaF/HCl, or ammonium bifluoride (NH_4HF_2), which act as alternative etchants [51]. These compounds generate HF in situ within the solution, facilitating the etching of the MAX phase. Notably, in addition to extracting the A atoms and forming surface-functionalized $M_nX_{n-1}T_m$ layers, this modified approach allows the intercalation of various cations and even neutral molecules, including Li^+, Na^+, K^+, NH^{4+}, tetrabutylammonium (TBA), and N,N-dimethylformamide, into the interlayer spaces [52]. This intercalation weakens the interlayer interactions and, in turn, promotes the delamination process. However, these methods typically require several hours to days to synthesize MXenes, leading to reduced production efficiency and increased costs [53]. Furthermore, the inherent corrosiveness and toxicity of HF pose significant challenges to experimental safety and scalability.

3.2. Fluoride-Free Etching Routes

The high toxicity and corrosiveness of fluoride limit the large-scale production and development of MXenes. To overcome the hazards associated with fluoride-based etching, researchers have explored fluoride-free solutions for MXene etching [54]. Current fluoride-free etching methods include alkali-assisted treatment and electrochemical etching, both of which have been introduced as alternatives for synthesizing fluoride-free MXenes.

3.2.1. Alkali-Assisted Treatment

Leveraging the amphoteric nature of the A layer atoms in MXenes, Li et al. [55] pioneered an alkali-assisted hydrothermal method to produce accordion-like, fluoride-free $Ti_3C_2T_x$. During the etching process, hydroxide (OH^-) ions from the alkali solution exhibit a similar etching effect to fluoride ions in acid etching, with the Al layer being attacked by OH^- and dissolving into soluble $Al(OH)_4^-$ in a NaOH solution. The $Ti_3C_2T_x$ MXene produced by NaOH etching exhibits a similar accordion-like structure to that obtained by HF etching, with -O and -OH terminal groups on the surface, and good hydrophilicity. Compared to HF, NaOH presents a lower risk; however, the high demands on the concentration of the alkaline solution and processing temperature limit its scalability for large-scale applications [56].

3.2.2. Electrochemical Etching

Electrochemical etching is another selective etching technique, which requires careful selection of the electrolyte. For certain MAX phase materials, such as Ti_3AlC_2, electrochemical etching in dilute NaCl, HCl, or HF solutions can lead to the corrosion of the entire material. Considering the strong binding between Cl^- and Al, Feng et al. [57] chose a binary aqueous electrolyte with a pH greater than 9 (1 M NH_4Cl and 0.2 M tetramethylammonium hydroxide (TMAOH), pH > 9) to electrochemically etch Ti_3AlC_2, successfully preparing $Ti_3C_2T_x$. During electrochemical etching, Al atoms are extracted by Cl^- anions, which disrupt the Ti-Al bonds, selectively etching the Al layer. The subsequent intercalation of OH^- promotes the formation of fewer-layer and single-layer nanosheets. However, since MAX phases often exist in dense bulk forms, only the surface is in contact with the electrolyte during electrochemical etching. Over time, this can lead to the formation of a three-layer structure, with MXA phase cores, intermediate MXenes, and carbide-derived carbon, making MXene collection difficult and significantly reducing the yield. The addition of appropriate intercalants can help expand the interlayer spacing, further enhancing the etching efficiency and yield of MXenes.

3.3. Molten Salt Etching

3.3.1. Molten Fluoride Salt Etching

In contrast to carbide MXenes, the aluminum atoms in nitride MXenes bind more strongly to the metal (M) and require higher energy for removal. Furthermore, the M-X bond stability in nitrides is relatively low, and during etching, Ti_nN_{n-1} may dissolve in HF solution, making traditional methods unsuitable [58]. To address these challenges, researchers have employed fluoride-containing low-melting salts (e.g., KF, LiF, NaF) in combination with Ti_4AlN_3 at 550 °C, successfully producing $Ti_4N_3T_x$ with surface groups such as -F and -O [59]. However, this method requires high temperatures, and the resulting MXenes exhibit low crystallinity, with an excessive number of defects and vacancies. Additionally, the large amount of -F groups grafted onto the MXene surface in traditional fluoride etching methods may impede ion diffusion, thereby compromising the performance of energy storage devices. Despite these limitations, molten salt etching has opened a new avenue for synthesizing various MXenes, including fluoride-free approaches for MXenes.

3.3.2. Lewis Acid Molten Salt Etching

To mitigate the hazards associated with fluoride etching, a Lewis acid molten salt etching method has been proposed as an alternative to traditional HF-based solvents for MXene synthesis. This technique involves a redox coupling between the A element and the cations of the Lewis acid molten salts to etch the MAX phase [60]. Currently, this approach applies to the synthesis of various MXenes from non-traditional MAX phase precursors containing A elements, such as silicon, zinc, and gallium [61]. The key advantage of this method is its ability to uniformly functionalize the Tx groups in the MXene layers. MXenes produced via this method exhibit weaker terminal group bonding, allowing for substitution and elimination reactions that enable the preparation of MXenes with specific or even no terminal groups (bare MXenes). This offers promising prospects for tuning the properties and applications of MXenes. However, high reaction temperatures and energy consumption, along with the difficulty in delaminating MXenes into single layers, are still challenges. Moreover, this method is still in its exploratory phase, and further research is needed to evaluate the conductivity, hydrophilicity, and other properties of the resulting MXenes.

3.4. Other Etching Methods

The methods discussed above are predominantly top–down approaches, where MXenes are derived by delaminating layered parent compounds (MAX phases) through harsh etching steps. These methods are primarily applicable to MAX phases with aluminum layers in the A site. In contrast, chemical vapor deposition (CVD) is a bottom–up synthesis technique that involves the reaction of gaseous precursors on a substrate to form films, heterostructures, and complete devices. Wang et al. [7]. utilized CVD to synthesize Ti_2CCl_2, an MXene that cannot be obtained from MAX phases. This method uses methane and titanium (Ti) tetrachloride to react on the Ti surface, resulting in Ti_2CCl_2 flakes oriented vertically to the metallic substrate. This alignment facilitates rapid ion intercalation/de-intercalation, promoting the development of MXenes for high-power battery anodes. The MXenes grown by CVD exhibit carpet-like and complex spherical morphologies, which enhance the exposure of active surface sites, further facilitating ion intercalation/de-intercalation [62]. However, the high temperature and low yield associated with this method limit its commercial scalability. Additionally, ion sputtering has been used to synthesize ultra-thin Ti_2C nanosheets. A low-energy heavy ion beam is directed at a target to bombard Ti and C, resulting in the formation of repetitive nanoscale layers of a single phase [63]. While these two methods (CVD and ion sputtering) produce MXenes with no terminal groups on their surfaces, they typically suffer from low yields and high equipment requirements.

4. Issues of MXenes

In the domain of electrochemical energy storage, MXenes, a class of 2D materials, have gained considerable attention due to their exceptional electrochemical properties [64]. Their distinctive layered structure, high electrical conductivity, and large specific surface area offer significant potential for applications in energy storage devices, such as supercapacitors and batteries [65]. Despite these promising characteristics, MXenes face several critical challenges that hinder their practical implementation, as shown in Figure 3. The following discusses the key issues and potential solutions:

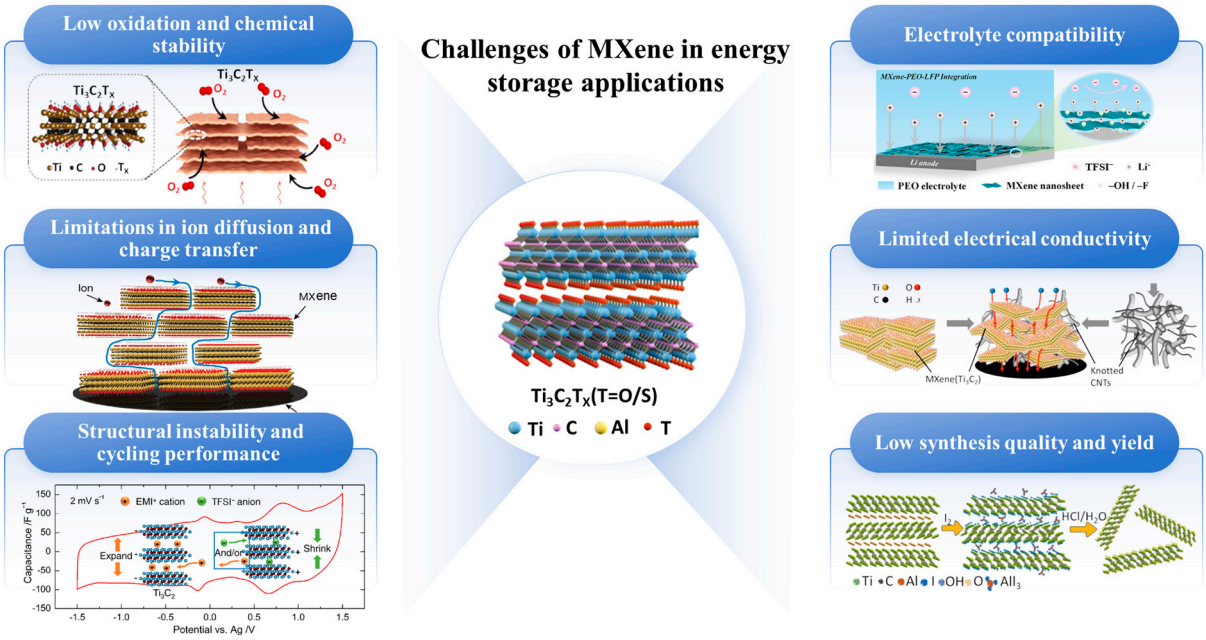


Figure 3. Overview of the challenges faced by MXenes in the realm of electrochemical energy storage.

4.1. Prone to Oxidation

MXenes possess surface functional groups, including -OH, -O, and -F, which contribute to their excellent hydrophilicity and electrochemical reactivity [66]. However, these functional groups also make MXenes vulnerable to environmental factors, particularly oxidation. Exposure to humid air, oxygen, or electrolytes can lead to alterations in the surface chemistry, causing the loss of metal elements and the formation of unstable oxides. This oxidation process can result in significant degradation, affecting both conductivity and electrochemical performance and, ultimately, compromising cycle stability. Therefore, enhancing the chemical stability of MXenes, while preserving their superior electrochemical properties, remains a key research focus. Solutions such as surface passivation, alloying, or the use of protective coatings have been proposed to mitigate these issues.

4.2. Limitations in Ion Diffusion and Charge Transfer

While MXenes exhibit a high specific surface area, their layered structure imposes limitations on ion diffusion between layers. This becomes particularly problematic under high rate charge and discharge conditions, where the restricted ion transport negatively impacts the performance of MXenes in high-power applications, like supercapacitors, which demand rapid ion movement [67,68]. To overcome this limitation, various strategies have been explored, such as optimizing the interlayer structure, designing porous frameworks, and combining MXenes with conductive materials to enhance ion diffusion and charge transfer, thereby improving the electrochemical performance [69].

4.3. Structural Instability

The inherent layered structure of MXenes, while beneficial for electrochemical performance, also leads to issues with structural stability. During repeated charge–discharge cycles, MXenes undergo expansion and contraction, which can result in the peeling or collapse of the material, leading to the loss of active sites and a reduction in capacity and cycle life [70]. This structural instability is exacerbated under high rate cycling conditions. To address this, surface modification, composite material design, and the development of advanced synthesis methods have been proposed to enhance the mechanical strength of MXenes and prevent degradation during long-term use [71].

4.4. Electrolyte Compatibility

The interaction between MXenes and electrolytes significantly influences their electrochemical properties. In certain electrolytes, the surface functional groups of MXenes may react with ions, leading to modifications in the surface chemistry, which can compromise material stability and battery performance [72,73]. Moreover, high-voltage conditions may induce adverse reactions between MXenes and electrolyte components, generating byproducts that compromise the safety and longevity of the battery [74]. Solutions to these challenges include developing electrolytes compatible with MXenes or modifying their surface properties to improve compatibility with various electrolytes. Additionally, optimizing electrolyte pH, conductivity, and solvent composition can further enhance MXene–electrolyte interactions [75].

In conclusion, while MXenes hold substantial promise in the field of electrochemical energy storage, their practical applications are still limited by several challenges. Advancements in synthesis methods, surface modification strategies, composite material design, and electrolyte compatibility optimization are essential to improving the performance of MXenes and facilitating their widespread use in energy storage devices.

4.5. Limited Conductivity

Although MXenes exhibit intrinsic metallic conductivity, owing to their metallic bonds and 2D structure, their electrochemical performance can be compromised in high-power applications, particularly during rapid charge/discharge cycles. At elevated current densities, the inherent conductivity of MXenes may not be sufficient to support efficient electron transport, leading to significant degradation in power output and capacity. This limitation arises from the fact that, while MXenes are locally conductive, interlayer interactions and the absence of a continuous conductive network impede electron flow during high-rate cycling [76]. To address this challenge, enhancing the conductivity of MXenes is paramount. Strategies such as composite formation with other conductive materials (e.g., graphene or carbon nanotubes) and the optimization of the conductive network can improve electrochemical performance [77]. Additionally, reducing interlayer van der Waals forces via surface engineering may facilitate the mobility of both ions and electrons, thereby enhancing the overall conductivity and enabling MXenes to meet the stringent demands of high-performance applications, such as electric vehicles and high-rate supercapacitors.

4.6. Low Synthesis Quality and Yield

Current synthesis methods for MXenes often rely on highly corrosive chemical reagents, such as HF, HCl, and NaOH, which can lead to low-quality MXenes with reduced specific surface area, suboptimal conductivity, and poor electrochemical performance [78]. Furthermore, although high-frequency etching can effectively exfoliate MXenes, this process generates hazardous waste, posing environmental and safety risks, and complicates large-scale production [79]. Therefore, the development of simple, cost-effective, and sus-

tainable synthesis routes, coupled with the ability to achieve uniformity and high yields in large-scale production, is key to advancing the commercial viability of MXenes.

5. Functional Modification of MXenes and Their Applications in Electrochemical Energy Storage

To overcome the challenges that MXene materials face in electrochemical energy storage applications—such as structural instability, limited conductivity, and insufficient cycle life—various functionalization approaches have been proposed, including surface chemical modification, doping, intercalation, and the creation of composites (Figure 4). These strategies aim to enhance the electrochemical performance, stability, and overall versatility of MXenes. Surface chemical modifications, for instance, allow for the tailoring of functional groups on the MXene surface, facilitating improved ion and electron transport. Doping and intercalation techniques alter the interlayer spacing and electronic structure of MXenes, thereby optimizing their conductivity and charge storage capacity. Furthermore, the incorporation of MXenes into composites with other high-performance materials enhances their functional characteristics. Collectively, these functionalization approaches offer a promising pathway for advancing MXene-based materials, expanding their applicability in the next generation of energy storage technologies.

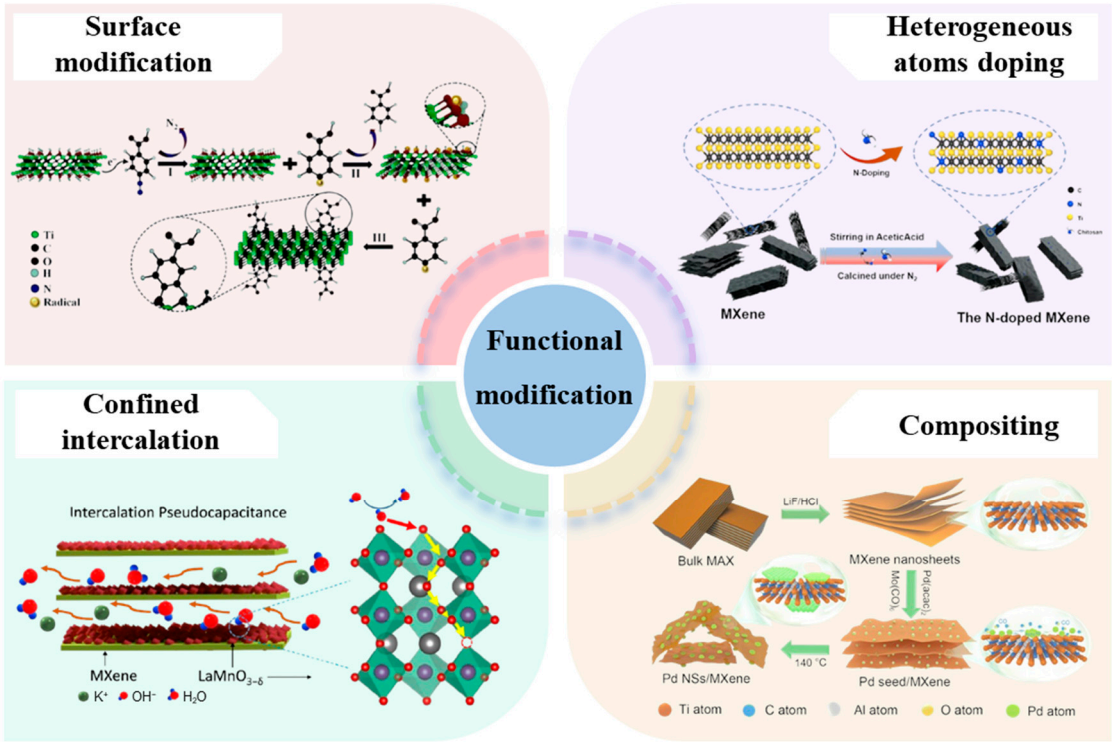


Figure 4. Diverse strategies for the functional modification of MXene materials.

5.1. Surface Chemical Modification of MXenes

The rich surface functional groups present on MXenes allow for performance modulation through functional group adjustments. Most theoretical calculations suggest that these surface groups play a crucial role in determining the hydrophilicity, stability, and other physicochemical properties of MXenes. Early studies have shown that, among the conventional terminal groups of MXenes (i.e., -O, -OH, -F), the O-terminal group contributes the most to lithium storage capacity, while -OH and -F terminals are less favorable for lithium storage due to their poor conductivity [80,81]. However, in practical applications, such as capacitors or other energy storage devices, MXenes primarily store energy through

ion or molecular adsorption and desorption, generating double-layer capacitance, as well as pseudocapacitance from redox reactions based on Ti elements, along with changes in interlayer spacing during charge and discharge cycles. The traditional functional groups mentioned above are unable to provide substantial energy storage contributions, thus hindering the balance between high capacity and long cycle stability.

In contrast to conventional terminal groups, P is considered a promising substitute due to its low electronegativity and rich valence state variations, offering the potential to simultaneously enhance both capacity and stability. Based on this concept, Zhu et al. [82] developed a $Ti_3C_2PBr_x$ MXene with P-functional groups via a two-step gas etching/functional group substitution method, which was applied to supercapacitors. As shown in Figure 5a, the Ti_3AlC_2 MAX phase was first etched using Br_2 gas to directly obtain $Ti_3C_2Br_2$ MXene powder. Subsequently, P vapor was introduced to replace the Br terminal with P, while H_2 gas was used to prevent the oxidation and phase transformation of the MXene. The formation of PBr_3 vapor significantly reduced the secondary reversible substitution of Br and further converted the vapor into PBr_3 liquid, increasing the P substitution ratio. Notably, the method involved four different temperature zones, each corresponding to distinct reactions, as depicted in Figure 5b. Tests and analysis of the charge/discharge process of $Ti_3C_2PBr_x$ MXene indicated that the introduction of the P-functional group effectively enhanced the pseudocapacitance of the material due to the formation of redox-active sites between the P group and Ti. Classical molecular dynamics simulations further showed that H_3O^+ ions accumulated more on the $Ti_3C_2PBr_x$ surface compared to $Ti_3C_2Br_2$, which promoted greater involvement of H_3O^+ in pseudocapacitive reactions. Therefore, $Ti_3C_2PBr_x$ MXene materials exhibit great potential for application in supercapacitor devices. Similarly, Wang et al. [83] proposed a novel molten-salt-assisted electrochemical etching method (MS-E-etching) to synthesize fluorine-free $Ti_3C_2Cl_2$. This method utilizes electrons as a reaction medium, spatially separating cathodic reduction and anodic etching processes. For the MS-E etching mechanism, the density functional theory (DFT) was employed to calculate the electronic properties and chemical adsorption energy of Cl- anions on the Ti_3AlC_2 (100) surface, which was used to explain the etching mechanism, as shown in Figure 5c. By adding various inorganic salts, the surface functional groups of MXenes were modified in situ, changing the terminal groups from -Cl to -O and/or -S, thereby significantly shortening the modification process and enriching the variety of surface terminal groups. The fabricated O-functionalized $Ti_3C_2T_x$ MXene exhibited high specific capacitance, excellent rate performance, and remarkable cycling stability at a current density of 1.0 A g^{-1}, outperforming the multilayer $Ti_3C_2T_x$ MXene electrodes synthesized by other etching methods.

Despite the excellent surface chemistry and conductivity of 2D MXenes terminated with functional groups, additional surface modifications are required to achieve various desired properties, such as antioxidation, hydrophobic surfaces, and efficient ion transport. To meet these requirements, small-molecule organic compounds are utilized to functionalize 2D MXenes, where the interaction between the terminal functional groups on the MXenes and functional groups on the organic compounds plays a key role. For instance, Kim et al. [84] reported a method for the stable dispersion of $Ti_3C_2T_x$ MXenes in nonpolar organic solvents using interface chemical grafting and phase transfer methods (Figure 6a). This approach involved nucleophilic addition reactions at the liquid–liquid interface between water and an organic solvent that is immiscible with water, followed by sequential condensation at room temperature, resulting in the chemical grafting of alkyl phosphonic acid ligands onto the hydroxyl terminal groups of $Ti_3C_2T_x$ sheets. This led to the formation of covalent Ti-O-P bonds and effectively functionalized the MXene. Due to the alkyl tail groups, the grafted $Ti_3C_2T_x$ exhibited strong antioxidative properties and long-term

stability in nonpolar organic solvents, making it a promising material for applications requiring both stability and functionalization. Additionally, Sun et al. [85] developed a high redox-active Nb_4C_3 MXene (referred to as PO_2-Nb_4C_3) by employing electrostatic self-assembly and terminal group conversion techniques (Figure 6b). The redox-active functional group PO_2^-, which mimics the structure of pyrophosphate, induced the creation of additional redox sites and significantly enhanced the redox depth of niobium. As a result, PO_2-Nb_4C_3 demonstrated a doubling of storage capacity compared to traditional -O-terminated Nb_4C_3 MXenes, exhibiting excellent fast charging rate performance and outstanding cycle stability. Inspired by the supramolecular interactions between amino acids in proteins, Guo et al. [86] modified MXene nanosheets through esterification reactions between the hydroxyl and carboxyl groups of serine to fabricate a self-healing nanostructured Ti_3C_2 MXenes/rubber-based supramolecular elastomer (NMSE) (Figure 6c). The NMSE material exhibited excellent flexibility and self-healing ability due to the hydrogen bonding interactions between the surface-modified $Ti_3C_2T_x$ and serine. This modification strategy offers a novel approach to enhancing the mechanical properties and functional performance of MXenes in energy storage and other advanced applications.

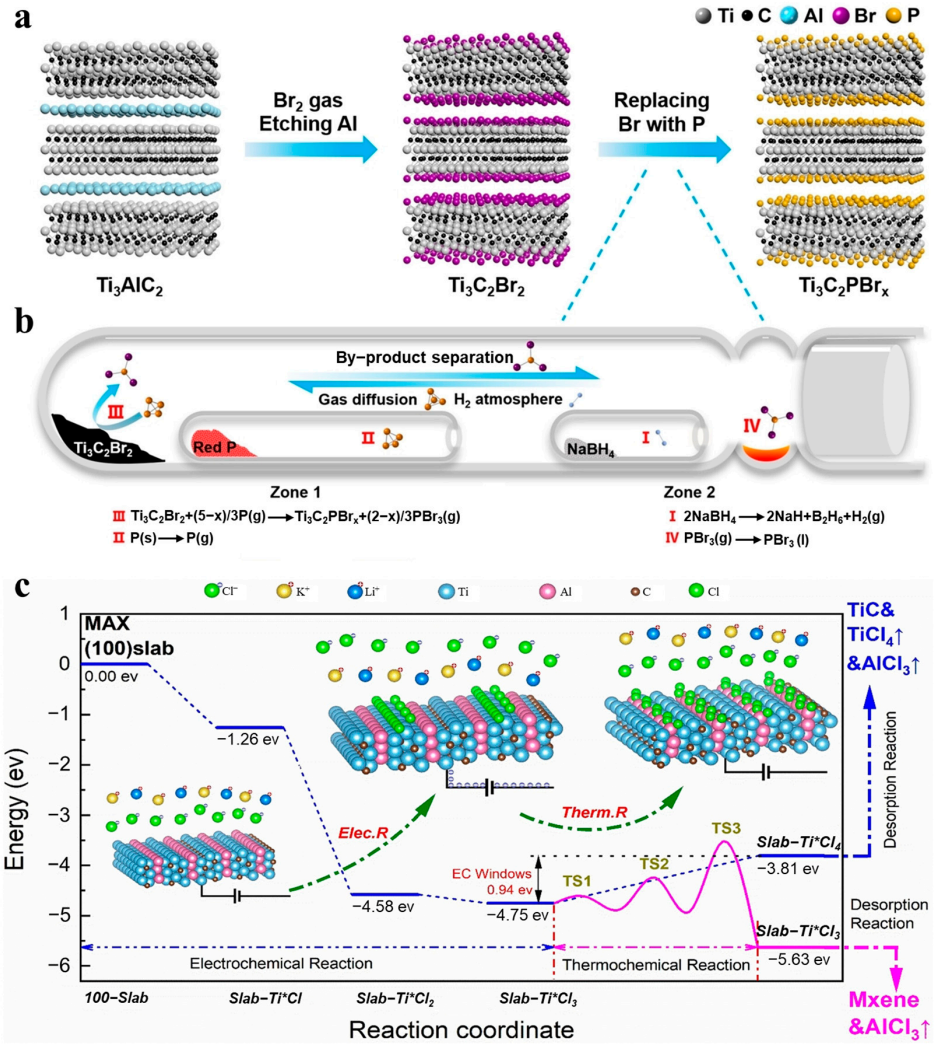


Figure 5. (**a**) Schematic illustration of the gas-phase preparation of MXene with -P functional groups. (**b**) Detailed mechanism for the substitution of -Br with -P functional groups. Panel (**a**,**b**) are reproduced with permission [82]. Copyright 2024, Wiley-VCH. (**c**) Reaction coordinate for the MS-E etching process of $Ti_3C_2T_x$. Reproduced with permission [83]. Copyright 2021, Wiley-VCH.

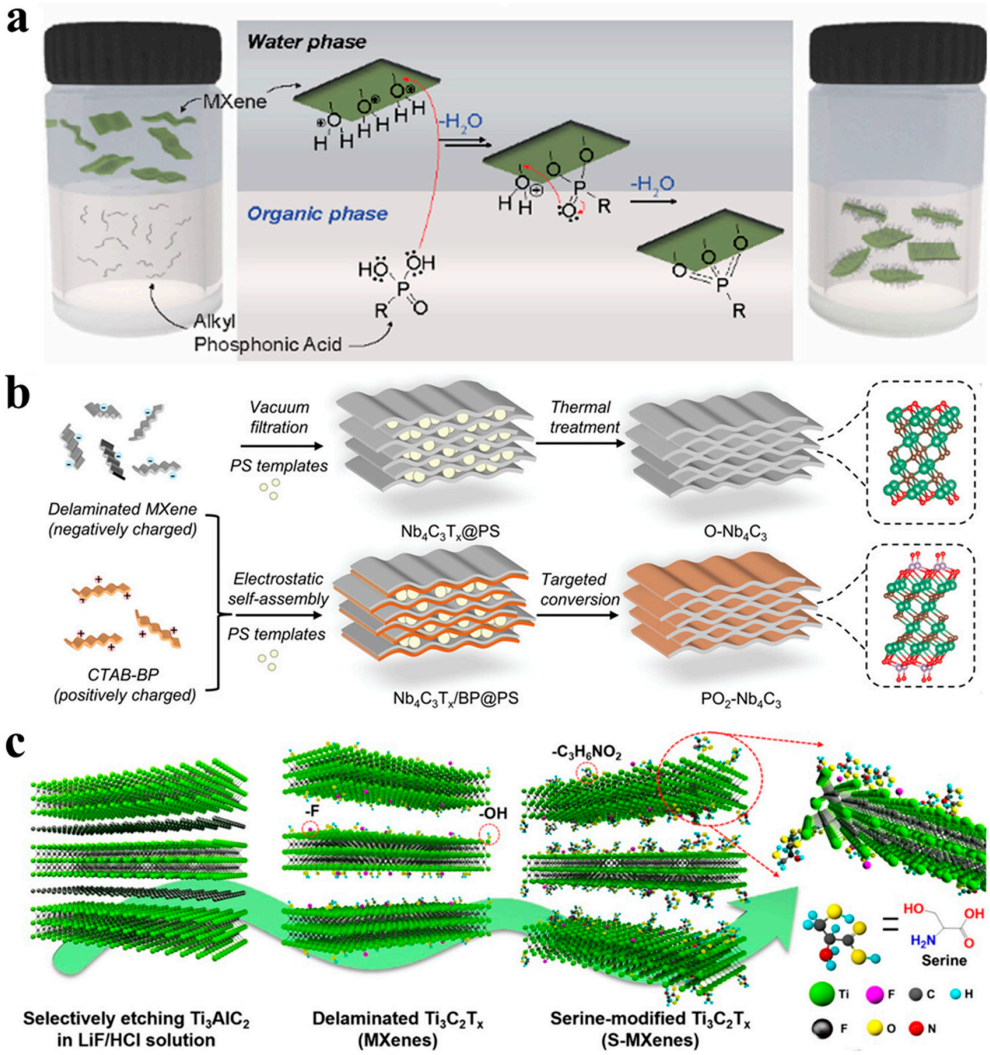


Figure 6. (**a**) Schematic illustration of simultaneous interfacial chemical grafting reaction and phase transfer for preparing a stable nonpolar $Ti_3C_2T_x$ dispersion. Reproduced with permission [84]. Copyright 2019, American Chemical Society. (**b**) Schematic illustration of the fabrication routes for O-Nb_4C_3 and PO_2-Nb_4C_3. Reproduced with permission [85]. Copyright 2022, Wiley-VCH. (**c**) Surface modification of MXene nanosheets by serine via the esterification reaction. Reproduced with permission [86]. Copyright 2020, American Chemical Society.

Based on the above discussion, different functional groups on MXenes play distinct roles in ion adsorption, electron transfer, and interface stability, contributing to the overall performance of materials in energy storage devices. Oxygen-based functional groups (such as -O and -OH) exhibit strong hydrophilicity, which promotes ion adsorption and enhances pseudocapacitance and ionic conductivity. However, they generally possess poor conductivity, limiting their high-performance capabilities in long cycle applications. Fluorine (-F) functional groups, although providing better hydrophobicity, restrict electron transfer due to their high electronegativity, resulting in poor performance in energy storage applications. In contrast, phosphorus (-P) is considered a promising alternative due to its lower electronegativity and versatile valence state changes, which can create redox-active sites. These sites not only enhance capacity but also improve stability, making phosphorus-functionalized MXenes highly suitable for applications requiring high capacity and long-term stability. Phosphorus functional groups also promote stronger ionic interactions, such as increasing the accumulation of H_3O^+ ions on the P-functionalized surface, further enhancing pseudocapacitive reactions. Chlorine (-Cl) functional groups

mainly contribute to interface stability by preventing oxidation but have limited impact on electron transfer and ion adsorption. This makes chlorine-functionalized MXenes more suitable for structural stabilization rather than enhancing energy storage capabilities. Additionally, surface modification using small organic molecules (such as alkylphosphonic acids) can improve antioxidant properties and dispersion in non-polar solvents, thereby expanding the functionality of MXenes. In summary, oxygen-based functional groups facilitate ion adsorption and charge transfer, phosphorus-based functional groups provide a superior balance of capacity enhancement and long-term stability, while chlorine offers stability at the expense of performance. Organic modifications can further optimize these materials, improving their mechanical properties and chemical stability. Therefore, the choice of functional groups depends on the specific performance requirements of energy storage devices.

5.2. Doping

Unlike surface chemical modification, doping refers to the strategy of introducing foreign atoms into a material to create defects that can modulate its properties. By doping MXene materials with foreign atoms, defect-rich high-activity sites can be generated, offering additional charge storage sites and inducing local lattice distortions to regulate the atomic coordination environment, thereby optimizing their electronic structure and charge transfer characteristics. For instance, Jian et al. [87] employed nitrogen atoms with strong electronegativity and pseudocapacitance properties to dope the $Ti_3C_2T_x$ MXene with a distinct layered structure. Through a hydrothermal synthesis strategy, they introduced $C_2N_3^-$ anions into the interlayers and surfaces of $Ti_3C_2T_x$ MXenes, leading to the in-situ trimerization of these anions and the formation of stable $C_6N_9^{3-}$ ions (Figure 7a). The resulting $Ti_3C_2T_x/Na_3TCM$ exhibited fast and efficient Na^+ storage capabilities. Additionally, when oxygen and fluorine atoms occupied the FCC sites on the Ti_3C_2 surface, the adsorption strength for Na^+ was significantly enhanced. After nitrogen doping, nitrogen atoms substituted fluorine atoms, forming the most stable sodium adsorption sites (Figure 7b). Moreover, nitrogen doping reduced the Na^+ diffusion barrier (≈0.03 eV) (Figure 7c), which further accelerated the diffusion rate of Na^+. This modification significantly enhanced the capacitance contribution of $Ti_3C_2T_x/Na_3TCM$ (Figure 7d), thereby improving its Na^+ storage capacity during rapid charge and discharge cycles.

Compared to N, P atoms exhibit lower electronegativity, which allows for a more substantial modulation of MXene structure and electrochemical activity. To explore this, An et al. [88] used triphenylphosphine as a P source to dope V_2CT_x through heat treatment. By controlling the annealing temperature, they were able to create P-doped V_2CT_x MXenes with controllable doping amounts and positions (Figure 7e). Their results demonstrated that, when the annealing temperature exceeded 300 °C, P atoms replaced vanadium vacancies, forming P-C bonds. The formation of P-C bonds effectively enhanced the electrocatalytic hydrogen evolution reaction (HER) kinetics of V_2CT_x MXenes, providing a novel strategy for improving the catalytic performance of MXene-based materials. Similarly, Tian et al. [89] reported that nitrogen doping increases the charge transfer resistance, thereby hindering the electron transfer kinetics of pseudocapacitive reactions. In contrast, p-type doping with boron (B) atoms can optimize electron transfer processes. Furthermore, the combination of B doping with vacancies enhances the electrochemical activity of MXenes, leading to an overall improvement in their performance. Experimental results show that B-doped MXene electrodes exhibit superior high-rate capability and volumetric capacitance. Additionally, the hybridization of B 2p and Ti 3d states near the Fermi level indicates that B doping alters the electronic structure, making the electron density around Ti ions more favorable for interaction with intercalated protons. This change enhances the adsorption

capability of protons on the MXene surface, while reducing the resistance to charge transfer within the material, thereby improving the efficiency of pseudocapacitive reactions. Recently, Song et al. [16] proposed that compared to single-element doping, dual-element doping can significantly enhance the chemical interactions between the atoms and the material. They successfully synthesized a wrinkled N, S co-doped functionalized MXene via a urea-induced pyrolysis method. Theoretical calculations confirmed that the dual-doping of nitrogen and sulfur shifted the d-band center of the transition metal Ti, which strengthened the adsorption and catalytic activity for LiPSs. Furthermore, the synergistic Lewis acid–base interactions between the dual-doped atoms and MXene significantly improved the cycling stability.

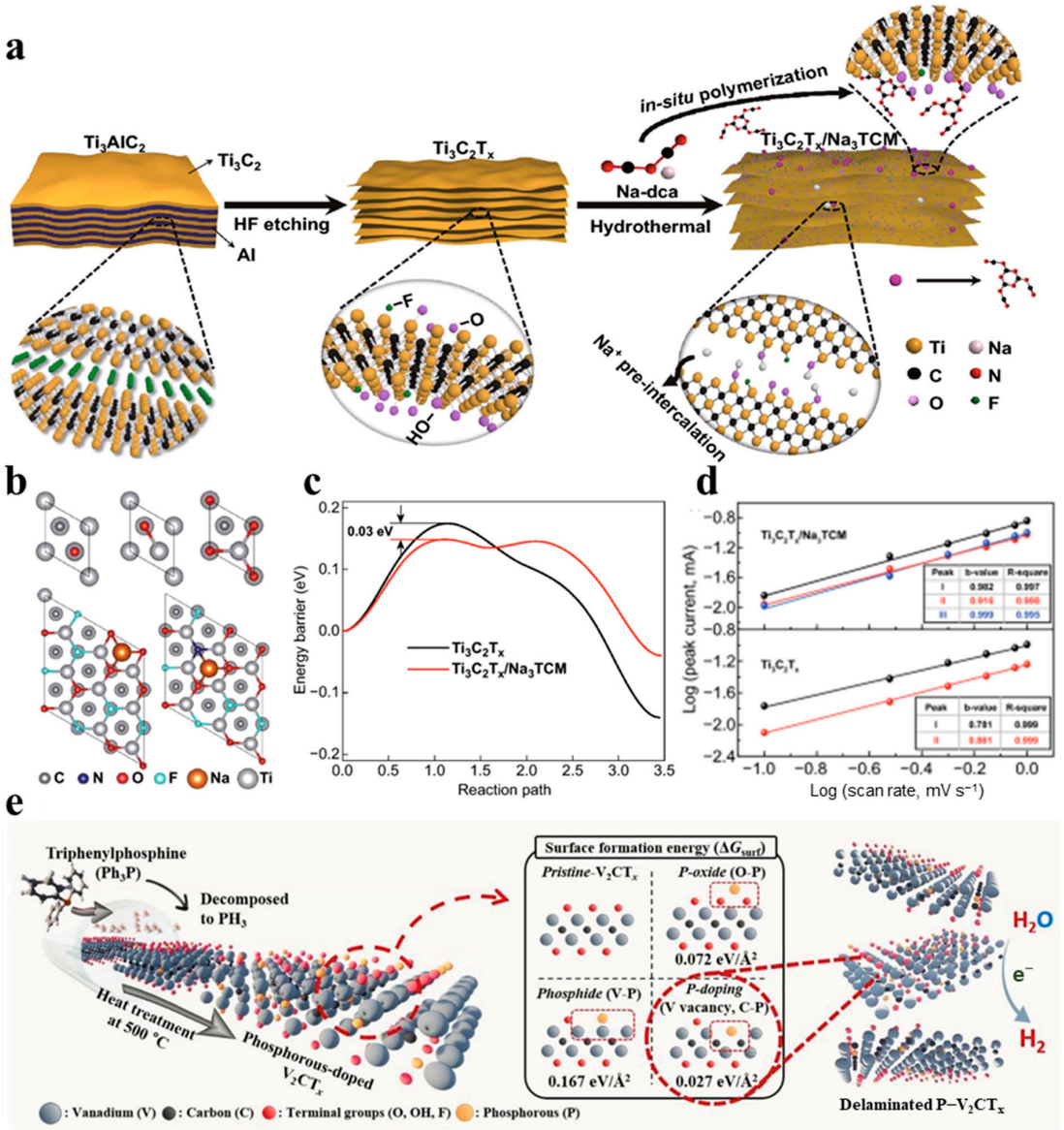


Figure 7. (**a**) Schematic illustration of the synthesis process for $Ti_3C_2T_x/Na_3TCM$, (**b**) DFT calculations for Na-ion storage on the $Ti_3C_2T_x/Na_3TCM$ and $Ti_3C_2T_x$ surfaces, (**c**) diffusion profiles of Na on the $Ti_3C_2T_x$ and $Ti_3C_2T_x/Na_3TCM$ surfaces as obtained from NEB calculations, (**d**) determination of the b values at the cathodic and anodic peak regions for $Ti_3C_2T_x/Na_3TCM$ (top) and $Ti_3C_2T_x$ (bottom). Panels (**a**–**d**) are reproduced with permission [87]. Copyright 2020, Springer Nature. (**e**) Schematic illustration of the phosphorization process for synthesizing P-doped V_2CT_x (P-V_2CT_x) nanosheets via heat treatment, along with their possible chemical compositions, which can be determined through calculated surface formation energy. Reproduced with permission [88]. Copyright 2019, Wiley-VCH.

Similarly, Liang et al. [90] proposed an interlayer domain restriction strategy by introducing ammonium polyphosphate (APP) between the $Ti_3C_2T_x$ MXene layers, followed by crosslinking to induce gelation and form a three-dimensional network structure, thereby increasing the interlayer spacing. Heat treatment was then applied to convert the crosslinked APP into nitrogen and phosphorus terminal groups on the $Ti_3C_2T_x$ MXene (Figure 8a). XPS spectra (Figure 8b) revealed that the main form of nitrogen in $Ti_3C_2T_x$/APP-A-3h was pyrrole nitrogen, which enhanced the redox reaction activity and electrochemical performance of MXenes. Moreover, phosphorus was primarily present in the form of P–O bonds, further improving the redox reaction ability and enhancing the pseudocapacitive performance (Figure 8c,d). DFT calculations indicated that, after nitrogen and phosphorus co-doping, the nitrogen atoms formed Ti–N bonds with Ti, while phosphorus atoms formed P–O bonds with oxygen. This co-doping modified the surface electronic state of the MXene, thereby increasing the conductivity of $Ti_3C_2T_x$ MXenes (Figure 8e). Benefiting from this interlayer confinement and N/P co-doping, $Ti_3C_2T_x$/APP-A-3h exhibited a higher surface capacitive contribution at various scan rates (Figure 8f). As a result, $Ti_3C_2T_x$ MXenes with N/P terminal groups demonstrated improved specific capacitance and cycling stability as supercapacitor electrodes (Figure 8g).

5.3. Intercalation

As mentioned earlier, the interlayer structure of MXene materials is held together by relatively weak van der Waals forces, which leads to stacking phenomena of the nanosheets. This severely hinders the effective exposure of active sites, thereby limiting the electrochemical activity of MXene materials. Therefore, it is essential to regulate the interlayer structure of MXenes to increase the interlayer spacing and alleviate the severe stacking problem. The intercalation strategy, which involves inserting guest species into the MXene interlayers to modulate their interlayer spacing, is considered an effective method for enhancing the electrochemical energy storage properties of MXenes. This approach typically involves introducing guest substances, such as molecules, atoms, ions, or solvents into the interlayer voids or van der Waals heterostructures of 2D materials like MXenes, thereby modulating material characteristics, such as interlayer interactions, electronic band structure, and Fermi level energy. Among the various types of intercalants, metal cations have demonstrated significant advantages due to their diverse types and tunable valency states.

Compared to ion intercalation, molecular intercalation allows for more precise control of the intercalation process, thereby effectively regulating the interlayer spacing of MXenes and optimizing the surface properties. For instance, Zheng et al. [91] employed four common intercalants—TMAOH, tetrabutylammonium hydroxide (TBAOH), dimethyl sulfoxide, and ethanol—to intercalate $Ti_3C_2T_x$ MXene (Figure 9a). Their study demonstrated that the intercalation strategy successfully expanded the interlayer spacing of MXene materials, its Raman spectroscopy confirmed the successful intercalation of four different intercalants into $Ti_3C_2T_x$ (Figure 9b), with TBAOH-MXene achieving an interlayer spacing of up to 16.58 Å. The introduction of these intercalants led to significant changes in the distribution of surface terminal groups on the MXenes. XPS analysis revealed that both TBAOH-MXene and TMAOH-MXene exhibited an increased presence of $-O$ and $-OH$ groups (Figure 9c). These modifications enhanced the hydrophilicity and electrochemical activity of the MXenes, thus improving their performance in energy storage applications. This increase in spacing effectively enhanced the ion diffusion rate between the layers during charge and discharge cycles, while simultaneously increasing the number of surface-active sites and improving the charge storage capacity. As a result, TBAOH-MXene exhibited excellent rate and cycling performance, with capacitance retention rates of 96.3% after 10,000 cycles at a scan rate of 50 mV s^{-1}, respectively (Figure 9d). However, despite the

improvements in electrochemical performance brought about by the introduction of these intercalants, challenges such as uncontrolled interlayer spacing and insufficient interfacial contact between different components may still hinder the ion diffusion efficiency during energy storage. Thus, maximizing the construction of monolayer MXenes and achieving precise guest material intercalation are key to significantly enhancing electrochemical energy storage properties. Dong et al. [92] further advanced this concept by co-assembling MXene $Ti_3C_2T_x$ nanosheets with Fe_3O_4 nanoparticles to incorporate conductive and porous components as pillar materials into the interlayers of 2D MXenes (Figure 9e), resulting in the synthesis of a multilayer MXene superlattice material with embedded monolayer mesoporous carbon frameworks (MMCF) ($Ti_3C_2T_x$/MMCF) (Figure 9f). Their research showed that the intercalated MMCF not only increased the interlayer spacing of the nanosheets but also created porous channels for fast ion transport. Additionally, the conductive pillars facilitated electron transfer along the z-direction. These unique structural features allowed the monolayer MXene to be fully utilized, enabling it to accommodate larger electrolyte molecules. Consequently, the $Ti_3C_2T_x$/MMCF superlattice exhibited exceptional performance in capacitive energy storage, particularly when tested in organic electrolytes containing high ion concentrations. The resulting micro-supercapacitors, fabricated from $Ti_3C_2T_x$/MMCF, achieved a 3.0 V voltage window and displayed high volumetric capacitance, surpassing most of the advanced MXene-based micro-supercapacitors developed to date.

The aforementioned intercalation strategies, by introducing various ions, molecules, and carbon materials into the MXene interlayers, have significantly improved the electrochemical performance of MXenes, especially in enhancing conductivity, capacity, and cycling stability. However, this strategy also has certain limitations, such as poor reversibility of the intercalated substances and stability issues between the interlayer regions, which may lead to performance degradation during long-term use. Therefore, the next section will explore MXene composite modifications, which, through the synergistic effects with other materials, further optimize the structural stability and electrochemical performance.

5.4. Hybridization with Other Materials

MXenes exhibit high redox capacitance and high specific surface area, making them highly attractive for energy storage devices that require high volumetric energy density. Despite the excellent conductivity and layered structure of MXenes, the performance of pure MXene materials in electrochemical energy storage devices is still limited by some inherent drawbacks, such as poor structural stability and limited ion storage capacity. To overcome these issues, researchers have been exploring the combination of MXenes with other conductive materials, metal materials, or transition metal compounds to create composite materials that take advantage of synergistic effects, thereby enhancing energy density, cycling stability, and power density of the electrodes. For example, Gogotsi et al. [93] employed atomic layer deposition (ALD) to grow oxides on 2D Ti-MXene sheets to prepare SnO_2/MXene composite anodes (Figure 10a). This composite electrode not only utilizes the high lithium-ion capacity of SnO_2 but also maintains the structural and mechanical integrity of the MXene platform. Therefore, as a lithium-ion battery anode, the conductive MXene/SnO_2 sheets can buffer the volume changes that occur during lithiation and delithiation processes, exhibiting excellent electrochemical performance. Based on this, the HfO_2-passivated SnO_2/MXene electrodes further improve the structural integrity of the SnO_2/MXene anode during cycling. As a result, the composite anode demonstrates a stable specific capacity of up to 843 mAh g^{-1}. Wang et al. [94] utilized an H^+-induced electrostatic self-assembly method to construct a hollow Fe_3O_4/C microsphere with inherent positive charges and few-layer MXene with inherent negative charges, thereby forming

the Fe_3O_4/C@MXene composite structure (Figure 10b). XPS characterization results indicated that the spinel-structured Fe_3O_4 exhibited a mixed Fe^{2+}/Fe^{3+} ratio, confirming its mixed valence state. Furthermore, Fe_3O_4 was successfully in situ encapsulated within an amorphous carbon matrix (Figure 10c). This encapsulation effectively protected Fe_3O_4 from degradation, thereby enhancing the stability and electrochemical performance of the composite material. The uniform and interconnected Fe_3O_4/C@MXene composite structure significantly promotes the rapid diffusion of Li^+, smooth electron/charge transfer, and suppresses the pulverization of the material. As a result, the composite anode maintains an undegraded specific capacity of 907 mAh g^{-1} over long-term cycling and demonstrates high energy density and cycling stability when applied in a 4.0 V lithium-ion capacitor (Figure 10d).

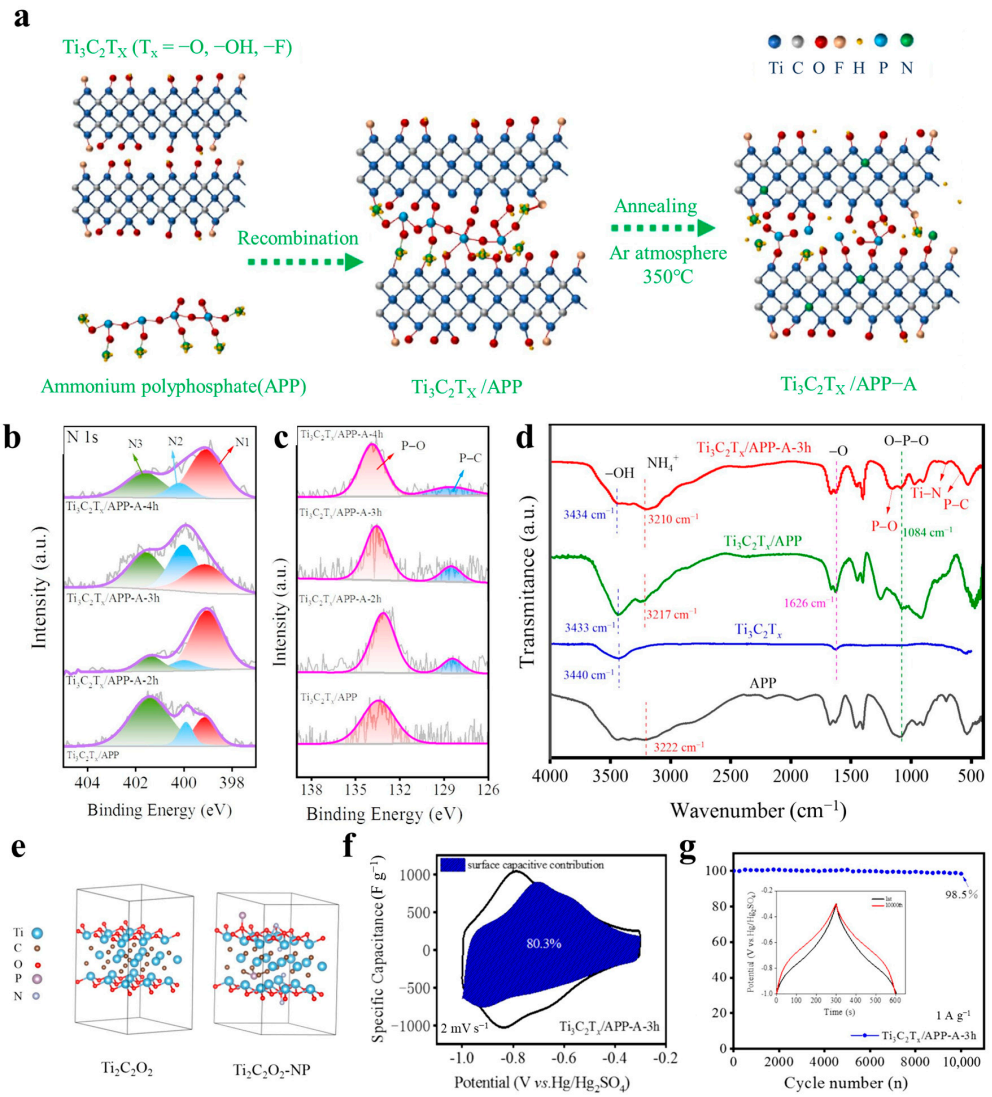


Figure 8. (**a**) Schematic diagram of nitrogen and phosphorus doping principle of $Ti_3C_2T_x$. (**b**) High-resolution N 1s spectra. (**c**) High-resolution P 2p spectra of $Ti_3C_2T_x$/APP, $Ti_3C_2T_x$/APP-A-2h, $Ti_3C_2T_x$/APP-A-3h, and $Ti_3C_2T_x$/APP-A-4h. (**d**) FTIR spectra of APP, $Ti_3C_2T_x$, $Ti_3C_2T_x$/APP, and $Ti_3C_2T_x$/APP-A-3h. (**e**) Model structure of $Ti_3C_2O_2$ and $Ti_3C_2O_2$-NP. (**f**) Surface capacitance contribution of $Ti_3C_2T_x$/APP-A-3h in the CV curve of 2 mV s^{-1}. (**g**) Cycling stability of $Ti_3C_2T_x$/APP-A-3h. Reproduced with permission [90]. Copyright 2024, Elsevier.

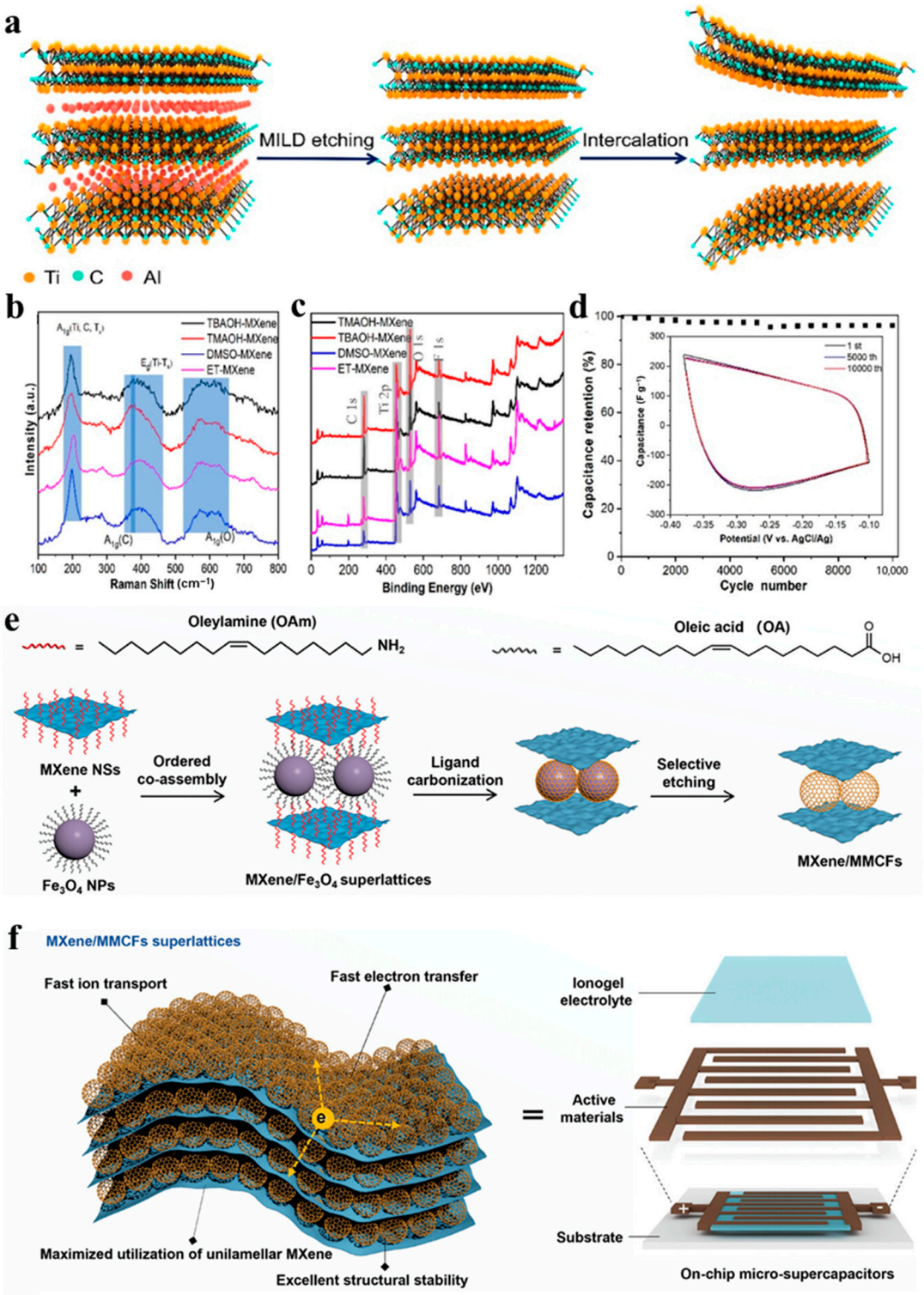


Figure 9. (**a**) Schematic illustration of MXene preparation and intercalation. (**b**) Raman spectra of TBAOH-MXene, TMAOH-MXene, DMSO-MXene, and ET-MXene under excitation with a 532 nm laser. (**c**) XPS survey spectra for TBAOH-MXene, TMAOH-MXene, DMSO-MXene, and ET-MXene. (**d**) Long-term cycling performance characterization curve of TBAOH-MXene after 1500, 5000, and 10,000 cycles at a scan rate of 50 mV s^{-1}. Reproduced with permission [91]. Copyright 2022, American Chemical Society. (**e**,**f**) Schematic illustration of (**e**) the fabrication of $Ti_3C_2T_x$/MMCFs and (**f**) the advantageous characteristics of $Ti_3C_2T_x$/MMCFs for supercapacitor applications. Panels (**e**,**f**) are reproduced with permission [92]. Copyright 2023, Wiley-VCH.

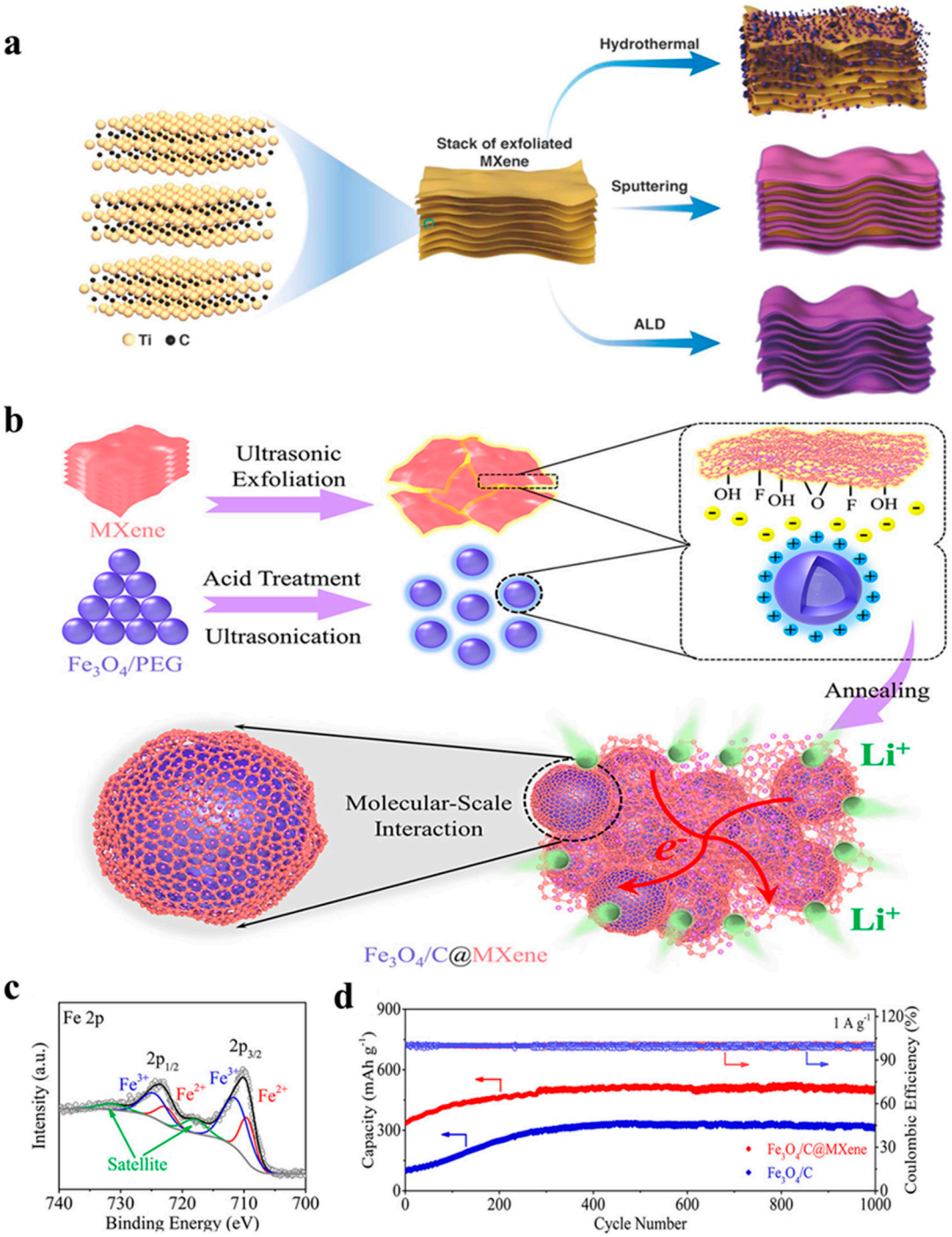


Figure 10. (**a**) Schematic representation of the various techniques employed for SnO_2 deposition onto Ti_3C_2 MXene sheets, encompassing hydrothermal synthesis, sputtering, and ALD. On the left, an atomic-scale depiction of exfoliated MXene sheets is shown, with a stack of these exfoliated sheets in the middle, and on the right, the MXene hybrid electrodes after SnO_2 deposition. (**b**) Typical fabrication process of electrostatically self-assembled Fe_3O_4/C@MXene nanocomposites. Reproduced with permission [94]. Copyright 2020, American Chemical Society. (**c**) XPS results of Fe 2p orbital spectra of Fe_3O_4/C@MXene nanocomposites. (**d**) Capacity retention and corresponding CE of Fe_3O_4/C@MXene and Fe_3O_4/C after 1000 GCD cycles. Reproduced with permission [93]. Copyright 2017, Elsevier.

Compared to TMOs, many transition metal sulfides (TMSs), such as NiS_x and CoS_x, exhibit higher electronic conductivity due to the lower electronegativity of sulfur compared to oxygen. This gives TMSs a higher specific capacity than their oxide counterparts

(e.g., NiO_x, CoO_x). However, TMSs often suffer from volume expansion during redox reactions, leading to rapid capacity decay and poor cycling stability in electrochemical energy storage applications. Hybridization and composite strategies with MXenes offer a potential solution to these issues. For instance, to improve the performance of nickel sulfide, Luo et al. [95] synthesized Ni-S/d-Ti_3C_2 nanohybrids via a simple solvothermal reaction (Figure 11a). The composite of d-Ti_3C_2 nanosheets with NiS not only prevented the aggregation of Ni-S nanostructures and alleviated their pulverization during cycling but also formed a synergistic interaction that enhanced the electron transport at the interface of the nanohybrid materials during charge/discharge processes. The XRD pattern demonstrated that the primary diffraction peaks of Ni-S/d-Ti_3C_2 corresponded with the typical peaks of the Ni-S phase. The (002) peak of d- Ti_3C_2 exhibited an increased interlayer spacing, which is beneficial for facilitating electrolyte ion diffusion (Figure 11b). Further confirmation came from XPS spectra, which indicated the interface interaction between Ni-S and d-Ti_3C_2 (Figure 11c). High-resolution Ni 2p spectra showed an increased Ni^{2+}/Ni^{3+}ratio (22.72% vs. 10.42%), promoting redox reactions (Figure 11d). Additionally, the slight left shift of the Ni 2p peak suggested the presence of chemical bonding between Ni-S and d-Ti_3C_2, optimizing the interface electronic structure and thereby enhancing the electrochemical activity of the composite. Furthermore, the re-stacking of d-Ti_3C_2 nanosheets was suppressed by the inserted Ni-S nanostructures, maintaining a larger active surface area. Consequently, the Ni-S/d-Ti_3C_2 nanohybrid exhibited significantly improved specific capacity and cycling stability compared to pure Ni-S materials. Similarly, Wang et al. [96] synthesized a highly stable 1T-MoS_2 nanosheet and Ti_3C_2 MXene composite with a three-dimensional interconnected microstructure. This 2D/2D heterostructure combined the collective advantages of 1T-MoS_2 nanosheets and Ti_3C_2 MXene, forming a robust synergistic interaction that effectively expanded the ion storage space, thereby enhancing capacitance. Additionally, due to the ultrafast electron transport from Ti_3C_2 MXene, the 1T-MoS_2/Ti_3C_2-based all-solid-state flexible symmetric supercapacitors exhibited outstanding rate performance. In a similar vein, MXene's excellent electronic and ionic conductivity, anisotropic charge mobility, and rich tunable surface functional groups make it an attractive candidate for composites with small molecules and organic materials. This approach has been widely explored to address the solubility and low conductivity issues of organic materials in organic electrolytes. The functional group interactions between $Ti_3C_2T_x$ MXene and organic materials can induce the polymerization and assembly of organic materials on the surface of the 2D MXene, resulting in uniform organic–inorganic hybrids, which is one of the common composite strategies. Gao et al. [97] successfully synthesized PAQS@$Ti_3C_2T_x$ MXene hybrids through hydrogen bonding and S-Ti interactions (Figure 11e). This hybrid exhibits a typical intercalated structure, with $Ti_3C_2T_x$ serving as an electronic and ionic transport channel, facilitating rapid charge and ion transfer. DFT calculations indicated that the introduction of MXene effectively reduced the adsorption energy of Na^+, promoting the reaction kinetics. As a result, the PAQS@MXene hybrid material demonstrated excellent sodium storage performance when used as a cathode in SIBs, exhibiting exceptional rate capability. It is noteworthy that the composite of MXene with organic materials has also enhanced its application in lithium–sulfur (Li-S), sodium–sulfur, and even, aluminum–sulfur batteries. This is because functional organic/MXene composite materials not only inhibit the shuttle effect but also improve conductivity/ionic conductivity and provide a high sulfur load due to the metallic conductivity and rich MXene terminal groups. For example, various organic materials, such as CTF, CTF/TNS, and Ti_3C_2@iCON, have been combined with MXene to form composites that serve as multifunctional sulfur host materials to enhance the performance of Li-S batteries [98,99].

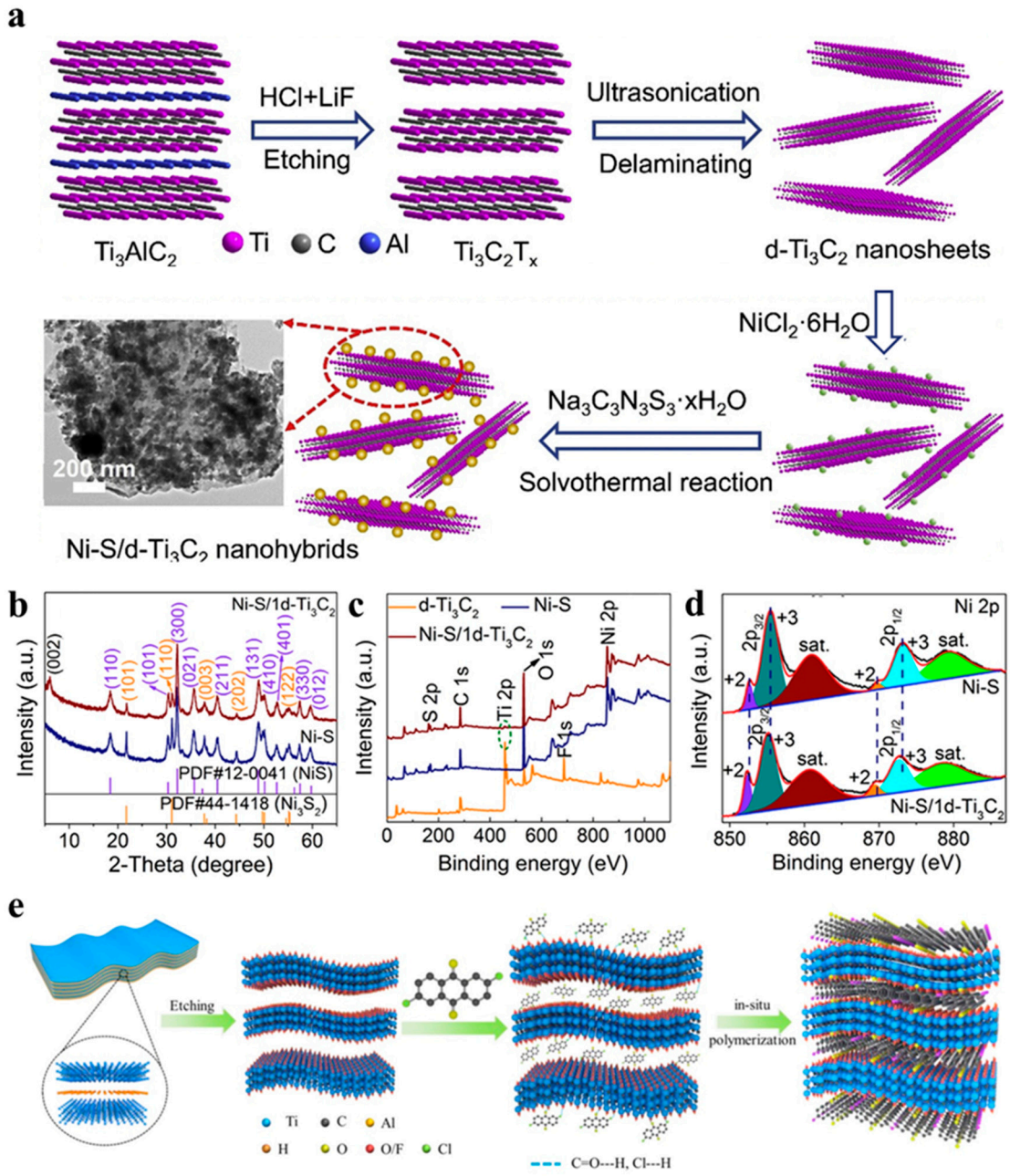


Figure 11. (**a**) Schematic diagram of the preparation methods for d-Ti_3C_2 nanosheets and Ni–S/d-Ti_3C_2 nanohybrids. (**b**) XRD patterns of Ni-S and Ni-S/1d-Ti_3C_2 nanohybrids. (**c**) XPS spectra of d-Ti_3C_2, Ni-S and Ni-S/1d-Ti_3C_2 nanohybrids. (**d**) High-resolution XPS spectra of Ni 2p in Ni-S and Ni-S/1d-Ti_3C_2 nanohybrids. Reproduced with permission [95]. Copyright 2020, Elsevier. (**e**) Schematic representation of the synthesis of PAQS@MXene hybrids. Reproduced with permission [97]. Copyright 2022, American Chemical Society.

In summary, the composite modification of MXene with other functional materials can effectively improve its electrochemical stability, ion transport rate, and cycling performance. In the future, precise control over the heterojunction structure and material combination of MXene-based composites will open up broader prospects for high energy density and long cycle life energy storage applications.

6. Conclusions and Perspectives

In conclusion, MXenes, with their unique structure, excellent conductivity, high surface area, and tunable surface chemistry, hold great potential for electrochemical energy

storage applications. These materials can offer high capacity, outstanding rate performance, and long-term cycling stability, making them ideal candidates for various energy storage systems, ranging from lithium-ion batteries to supercapacitors. However, several key challenges remain, limiting the widespread application of MXenes in this field. These include issues related to self-stacking, structural instability during cycling, and the scalability of functionalization methods. Functionalization strategies, such as surface chemical modification, doping, intercalation, and composite design, have made significant progress in enhancing the electrochemical and overall performance of MXene materials. These methods help improve ion/electron transport, extend cycling life, and mitigate material dissolution during operation. Nevertheless, precise control over the surface chemistry, interface interactions, and the structural integrity of MXenes during long-term cycling has not yet been fully achieved. Moreover, the energy storage mechanisms and multifunctional applications of MXenes in electrochemical energy storage still require further exploration. A deeper understanding of the interaction mechanisms between surface functional groups and the core MXene structure is crucial for advancing their applications in energy storage. Additionally, the scalability of synthesis methods needs to be addressed to produce MXenes with stable, high-quality characteristics that meet the requirements of electrochemical energy storage applications.

Therefore, future research should focus on the following key directions: (1) The development of scalable, green, and cost-effective synthesis methods for MXenes with controlled surface terminations and reduced defects. This includes exploring novel synthesis techniques, particularly molten salt methods, and investigating the selective etching of M-A bonds to support the development of environmentally friendly etchants. (2) Strengthening the study of the structural stability of MXenes and their functionalized products during charge/discharge cycles, particularly in long-term cycling processes. Research should focus on understanding degradation phenomena that may occur during storage and use and their dual effects on electrochemical performance, especially when using aqueous or aqueous/organic mixed electrolytes. (3) Investigating the complex ionic interactions between MXenes and electrolytes in electrochemical systems. The electrochemical behavior of MXene electrodes may vary depending on the intercalating ions and solvent environment. For instance, low ion conductivity electrolytes can provide maximum capacity and excellent rate performance in MXene electrodes. Moreover, MXenes exhibit battery-like behavior in ionic liquid electrolytes. Understanding the ionic interactions between MXenes and various electrolytes, as well as the corresponding energy storage mechanisms, will offer insights into the diverse ion storage pools and elucidate the influence of electrolyte environments on the electrochemical response and cycling stability of MXene electrodes. (4) In situ characterization and monitoring during operation. Advanced characterization techniques, such as synchrotron radiation, should be employed for in situ or operando studies of the electrochemical energy storage processes of MXenes and their functionalized counterparts. This will aid in clarifying and validating the role of functional groups, intercalation structures, and composite architectures in their energy storage mechanisms and electrochemical performance. (5) The multifunctional applications of MXenes in electrochemical energy storage devices. Expanding the use of MXenes in components, such as electrolytes, separators, and current collectors, while also imparting additional functions like catalytic activity, ion redistribution, and electrodeposition, will enhance their utility. Exploring the multiple roles of MXenes in energy storage devices, such as pseudocapacitance, redox reactions, and catalysis, can significantly improve the energy density, power density, and cycling life of batteries and supercapacitors. (6) The integration of theoretical calculations and experimental observations. To gain a deeper understanding of the mechanisms and structural evolution of electrode materials during energy storage processes, theoretical

calculation methods, such as density functional theory, molecular dynamics simulations, and finite element analysis, can be employed. These approaches can be used to study the electronic structure, ion diffusion pathways, interface interactions, and stability of MXenes. Computational simulations can predict the interaction mechanisms between the surface functional groups of MXenes and electrolyte ions, thereby optimizing material design and enhancing electrochemical performance. By addressing these challenges, MXenes have the potential to become transformative materials in the field of electrochemical energy storage, paving the way for the development of next-generation high-performance energy storage technologies.

Funding: This work was funded by National Natural Science Foundation of China (No. 52302223), the Fundamental Research Funds for the Central Universities (2232024G-06-01, 24S10102 and 23S10115), the Science and Technology Commission of Shanghai Municipality (24xtcx00300).

Conflicts of Interest: The authors declare no competing financial interest.

References

1. Dong, J.; Liu, Y.; Cui, Y. Emerging chiral two-dimensional materials. *Nat. Chem.* **2024**, *16*, 1398–1407. [CrossRef]
2. Chen, H.Y.; Chen, Z.Y.; Mao, M.; Wu, Y.Y.; Yang, F.; Gong, L.X.; Zhao, L.; Cao, C.F.; Song, P.; Gao, J.F. Self-adhesive polydimethylsiloxane foam materials decorated with MXene/cellulose nanofiber interconnected network for versatile functionalities. *Adv. Funct. Mater.* **2023**, *33*, 2304927. [CrossRef]
3. Roy, S.; Joseph, A.; Zhang, X.; Bhattacharyya, S.; Puthirath, A.B.; Biswas, A.; Tiwary, C.S.; Vajtai, R.; Ajayan, P.M. Engineered two-dimensional transition metal dichalcogenides for energy conversion and storage. *Chem. Rev.* **2024**, *124*, 9376–9456. [CrossRef]
4. Li, W.; Tao, Q.; Li, Z.; Yang, G.; Lu, Z.; Chen, Y.; Wen, Y.; Wang, Y.; Liao, L.; Liu, Y. Monolayer black phosphorus and germanium arsenide transistors via van der Waals channel thinning. *Nat. Electron.* **2024**, *7*, 131–137. [CrossRef]
5. An, Y.; Tian, Y.; Man, Q.; Shen, H.; Liu, C.; Xiong, S.; Feng, J. Fluorine-and acid-free strategy toward scalable fabrication of two-dimensional MXenes for sodium-ion batteries. *Nano Lett.* **2023**, *23*, 5217–5226. [CrossRef]
6. Li, B.; Wu, N.; Yang, Y.; Pan, F.; Wang, C.; Wang, G.; Xiao, L.; Liu, W.; Liu, J.; Zeng, Z. Graphene oxide-assisted multiple cross-linking of MXene for large-area, high-strength, oxidation-resistant, and multifunctional films. *Adv. Funct. Mater.* **2023**, *33*, 2213357. [CrossRef]
7. Wang, D.; Zhou, C.; Filatov, A.S.; Cho, W.; Lagunas, F.; Wang, M.; Vaikuntanathan, S.; Liu, C.; Klie, R.F.; Talapin, D.V. Direct synthesis and chemical vapor deposition of 2D carbide and nitride MXenes. *Science* **2023**, *379*, 1242–1247. [CrossRef]
8. Abraham, B.M.; Piqué, O.; Khan, M.A.; Viñes, F.; Illas, F.; Singh, J.K. Machine Learning-Driven Discovery of Key Descriptors for CO_2 Activation over Two-Dimensional Transition Metal Carbides and Nitrides. *ACS Appl. Mater. Interfaces* **2023**, *15*, 30117–30126. [CrossRef]
9. Lu, Q.; Liu, C.; Zhao, Y.; Pan, W.; Xie, K.; Yue, P.; Zhang, G.; Omar, A.; Liu, L.; Yu, M. Freestanding MXene-based macroforms for electrochemical energy storage applications. *SusMat* **2023**, *3*, 471–497. [CrossRef]
10. Yuan, T.; Zhang, Z.; Liu, Q.; Liu, X.-T.; Miao, Y.-N.; Yao, C.-L. MXene ($Ti_3C_2T_x$)/cellulose nanofiber/polyaniline film as a highly conductive and flexible electrode material for supercapacitors. *Carbohydr. Polym.* **2023**, *304*, 120519. [CrossRef]
11. Lu, C.; Li, A.; Zhai, T.; Niu, C.; Duan, H.; Guo, L.; Zhou, W. Interface design based on Ti_3C_2 MXene atomic layers of advanced battery-type material for supercapacitors. *Energy Storage Mater.* **2020**, *26*, 472–482. [CrossRef]
12. Zhang, W.; Jin, K.; Ren, Z.; Li, L.; Chang, L.; Zhang, C.; Wang, R.; Li, B.; Wu, G.; Hu, Y. High-Performance MXene/Carbon Nanotube Electrochemical Actuators for Biomimetic Soft Robotic Applications. *Adv. Funct. Mater.* **2024**, *34*, 2408496. [CrossRef]
13. Wang, Y.; Liu, L.; Wang, Y.; Qu, J.; Chen, Y.; Song, J. Atomically Coupled 2D MnO_2/MXene Superlattices for Ultrastable and Fast Aqueous Zinc-Ion Batteries. *ACS Nano* **2023**, *17*, 21761–21770. [CrossRef]
14. Zhou, Y.; Yang, J.; Zhou, N.; Hao, H.; Jiang, X.; Lei, F.; Shi, K.; Zhao, Y.; Zhou, G.; Liu, T. Amidoxime-functionalized MXene beads for the effective capture of uranium from wastewater with high fluoride concentrations. *Chem. Eng. J.* **2023**, *471*, 144647. [CrossRef]
15. Saraf, M.; Chacon, B.; Ippolito, S.; Lord, R.W.; Anayee, M.; Wang, R.; Inman, A.; Shuck, C.E.; Gogotsi, Y. Enhancing charge storage of $Mo_2Ti_2C_3$ MXene by partial oxidation. *Adv. Funct. Mater.* **2024**, *34*, 2306815. [CrossRef]
16. Feng, J.; Liu, W.; Shi, C.; Zhang, C.; Zhao, X.; Wang, T.; Chen, S.; Li, Q.; Song, J. Enabling fast diffusion/conversion kinetics by thiourea-induced wrinkled N, S co-doped functional MXene for lithium-sulfur battery. *Energy Storage Mater.* **2024**, *67*, 103328. [CrossRef]

17. Qian, H.; Peng, P.; Fan, H.; Yang, Z.; Yang, L.; Zhou, Y.; Tan, D.; Yang, F.; Willatzen, M.; Amaratunga, G. Horizontal Transport in $Ti_3C_2T_x$ MXene for Highly Efficient Osmotic Energy Conversion from Saline-Alkali Environments. *Angew. Chem. Int. Ed.* **2024**, *63*, e202414984. [CrossRef]
18. Cao, V.A.; Kim, M.; Lee, S.; Van, P.C.; Jeong, J.-R.; Park, P.; Nah, J. Chemically modified MXene nanoflakes for enhancing the output performance of triboelectric nanogenerators. *Nano Energy* **2023**, *107*, 108128. [CrossRef]
19. Ko, T.Y.; Ye, H.; Murali, G.; Lee, S.-Y.; Park, Y.H.; Lee, J.; Lee, J.; Yun, D.-J.; Gogotsi, Y.; Kim, S.J. Functionalized MXene ink enables environmentally stable printed electronics. *Nat. Commun.* **2024**, *15*, 3459. [CrossRef]
20. Shi, M.; Wang, R.; Li, L.; Chen, N.; Xiao, P.; Yan, C.; Yan, X. Redox-active polymer integrated with MXene for ultra-stable and fast aqueous proton storage. *Adv. Funct. Mater.* **2023**, *33*, 2209777. [CrossRef]
21. Zhang, Z.; Ying, H.; Huang, P.; Zhang, S.; Zhang, Z.; Yang, T.; Han, W.-Q. Porous Si decorated on MXene as free-standing anodes for lithium-ion batteries with enhanced diffusion properties and mechanical stability. *Chem. Eng. J.* **2023**, *451*, 138785. [CrossRef]
22. Jin, X.; Zhang, W.; Liu, S.; Zhang, T.; Song, Z.; Shao, W.; Mao, R.; Yao, M.; Jian, X.; Hu, F. Highly stable $Ti_3C_2T_x$ MXene-based sandwich-like structure via interfacial self-assembly of nitrogen-rich polymer network for superior sodium-ion storage performance. *Chem. Eng. J.* **2023**, *451*, 138763. [CrossRef]
23. Liu, Y.; Hong, X.; Liu, X.; Chen, W.; Tang, J. Electrolysis of seawater: An effective path to sustainable hydrogen production with sulfur-doped NiFe LDH/MXene@ NF electrodes. *Acs Sustain. Chem. Eng.* **2024**, *12*, 11520–11530. [CrossRef]
24. Du, Y.; Yan, Z.; You, W.; Men, Q.; Chen, G.; Lv, X.; Wu, Y.; Luo, K.; Zhao, B.; Zhang, J. Balancing MXene surface termination and interlayer spacing enables superior microwave absorption. *Adv. Funct. Mater.* **2023**, *33*, 2301449. [CrossRef]
25. Xu, Y.; Wang, F.; Lei, S.; Wei, Y.; Zhao, D.; Gao, Y.; Ma, X.; Li, S.; Chang, S.; Wang, M. In situ grown two-dimensional TiO_2/Ti_3CN MXene heterojunction rich in Ti^{3+} species for highly efficient photoelectrocatalytic CO_2 reduction. *Chem. Eng. J.* **2023**, *452*, 139392. [CrossRef]
26. Zeng, X.; Ye, Y.; Wang, Y.; Yu, R.; Moskovits, M.; Stucky, G.D. Honeycomb-like MXene/$NiFeP_x$–NC with" continuous" single-crystal enabling high activity and robust durability in electrocatalytic oxygen evolution reactions. *J. Adv. Ceram.* **2023**, *12*, 553–564. [CrossRef]
27. Khan, M.; Hussain, A.; Saleh, M.T.; Ibrahim, M.; Attique, F.; Sun, X.; Unalan, H.E.; Shafi, M.; Khan, Y.; Khan, I. Cutting-edge advancements in MXene-derived materials: Revolutionary electrocatalysts for hydrogen evolution and high-performance energy storage. *Coord. Chem. Rev.* **2024**, *506*, 215722. [CrossRef]
28. Javed, M.S.; Mateen, A.; Ali, S.; Zhang, X.; Hussain, I.; Imran, M.; Shah, S.S.A.; Han, W. The emergence of 2D MXenes based Zn-ion batteries: Recent development and prospects. *Small* **2022**, *18*, 2201989. [CrossRef]
29. Panda, S.; Deshmukh, K.; Pasha, S.K.; Theerthagiri, J.; Manickam, S.; Choi, M.Y. MXene based emerging materials for supercapacitor applications: Recent advances, challenges, and future perspectives. *Coord. Chem. Rev.* **2022**, *462*, 214518. [CrossRef]
30. Zhao, R.; Liu, C.; Zhu, Y.; Zou, G.; Hou, H.; Ji, X. Pathways for MXenes in Solving the Issues of Zinc-Ion Batteries: Achievements and Perspectives. *Adv. Funct. Mater.* **2024**, *34*, 2316643. [CrossRef]
31. Hussain, I.; Hanan, A.; Bibi, F.; Kewate, O.J.; Javed, M.S.; Zhang, K. Non-Ti (M_2X and M_3X_2) MXenes for Energy Storage/Conversion. *Adv. Energy Mater.* **2024**, *14*, 2401650. [CrossRef]
32. Patil, A.M.; Jadhav, A.A.; Chodankar, N.R.; Avatare, A.T.; Hong, J.; Dhas, S.D.; Patil, U.M.; Jun, S.C. Recent progress of MXene synthesis, properties, microelectrode fabrication techniques for microsupercapacitors and microbatteries energy storage devices and integration: A comprehensive review. *Coord. Chem. Rev.* **2024**, *517*, 216020. [CrossRef]
33. Cao, W.; Nie, J.; Cao, Y.; Gao, C.; Wang, M.; Wang, W.; Lu, X.; Ma, X.; Zhong, P. A review of how to improve $Ti_3C_2T_x$ MXene stability. *Chem. Eng. J.* **2024**, *496*, 154097. [CrossRef]
34. Cai, Y.; Chen, X.; Xu, Y.; Zhang, Y.; Liu, H.; Zhang, H.; Tang, J. $Ti_3C_2T_x$ MXene/carbon composites for advanced supercapacitors: Synthesis, progress, and perspectives. *Carbon Energy* **2024**, *6*, e501. [CrossRef]
35. Murali, G.; Reddy Modigunta, J.K.; Park, Y.H.; Lee, J.-H.; Rawal, J.; Lee, S.-Y.; In, I.; Park, S.-J. A review on MXene synthesis, stability, and photocatalytic applications. *ACS Nano* **2022**, *16*, 13370–13429. [CrossRef]
36. Cheng, Z.; Du, Z.; Chen, H.; Zhao, Q.; Shi, Y.; Wang, H.; Ye, Y.; Yang, S. Metal-Bonded Atomic Layers of Transition Metal Carbides (MXenes). *Adv. Mater.* **2023**, *35*, 2302141. [CrossRef]
37. Wei, C.; Tan, L.; Zhang, Y.; Xi, B.; Xiong, S.; Feng, J. MXene/organics heterostructures enable ultrastable and high-rate lithium/sodium batteries. *ACS Appl. Mater. Interfaces* **2022**, *14*, 2979–2988. [CrossRef]
38. Gao, P.; Song, M.; Wang, X.; Liu, Q.; He, S.; Su, Y.; Qian, P. Theoretical study on the electronic structure and magnetic properties regulation of janus structure of $M'MCO_2$ 2D MXenes. *Nanomaterials* **2022**, *12*, 556. [CrossRef]
39. Chowdhury, S.; Nugraha, A.S.; O'May, R.; Wang, X.; Cheng, P.; Xin, R.; Osman, S.M.; Hossain, M.S.; Yamauchi, Y.; Masud, M.K. Bimetallic metal-organic framework-derived porous one-dimensional carbon materials for electrochemical sensing of dopamine. *Chem. Eng. J.* **2024**, *492*, 152124. [CrossRef]

40. Kong, X.; Zong, X.; Lei, Z.; Wang, Z.; Zhao, Y.; Zhao, X.; Zhang, J.; Liu, Z.; Ren, Y.; Wu, L. A Universal In-Situ Interfacial Growth Strategy for Various MXene-Based van der Waals Heterostructures with Uniform Heterointerfaces: The Efficient Conversion from 3D Composite to 2D Heterostructures. *Small* **2024**, *20*, 2405174. [CrossRef]
41. Rems, E.; Hu, Y.-J.; Gogotsi, Y.; Dominko, R. Pivotal role of surface terminations in MXene thermodynamic stability. *Chem. Mater.* **2024**, *36*, 10295–10306. [CrossRef]
42. Ali, M.; Riaz, R.; Anjum, A.S.; Sun, K.C.; Li, H.; Jeong, S.H.; Ko, M.J. Graphene quantum dots induced porous orientation of holey graphene nanosheets for improved electrocatalytic activity. *Carbon* **2021**, *171*, 493–506. [CrossRef]
43. Zha, X.-H.; Yin, J.; Zhou, Y.; Huang, Q.; Luo, K.; Lang, J.; Francisco, J.; Du, S. Intrinsic Structural, Electrical, Thermal and Mechanical Properties of the Promising Conductor Mo_2C MXene. *J. Phys. Chem. C* **2016**, *120*, 15082–15088. [CrossRef]
44. Nandan, R.; Nara, H.; Nam, H.N.; Phung, Q.M.; Ngo, Q.P.; Na, J.; Henzie, J.; Yamauchi, Y. Tailored design of mesoporous nanospheres with high entropic alloy sites for efficient redox electrocatalysis. *Adv. Sci.* **2024**, *11*, 2402518. [CrossRef]
45. Kamysbayev, V.; Filatov, A.S.; Hu, H.; Rui, X.; Lagunas, F.; Wang, D.; Klie, R.F.; Talapin, D.V. Covalent surface modifications and superconductivity of two-dimensional metal carbide MXenes. *Science* **2020**, *369*, 979–983. [CrossRef]
46. Gentile, A.; Marchionna, S.; Balordi, M.; Pagot, G.; Ferrara, C.; Di Noto, V.; Ruffo, R. Critical analysis of MXene production with in-situ HF forming agents for sustainable manufacturing. *ChemElectroChem* **2022**, *9*, e202200891. [CrossRef]
47. Naguib, M.; Mashtalir, O.; Carle, J.; Presser, V.; Lu, J.; Hultman, L.; Gogotsi, Y.; Barsoum, M.W. Two-dimensional transition metal carbides. *ACS Nano* **2012**, *6*, 1322–1331. [CrossRef]
48. Zhang, X.; Zhang, W.; Zhao, H. Comparative study on fabrication and energy storage performance of $Ti_3C_2T_x$ MXene by using hydrofluoric acid and in situ forming of hydrofluoric acid-based approaches. *Int. J. Energy Res.* **2022**, *46*, 15559–15570. [CrossRef]
49. Gu, Q.; Cao, Y.; Chen, J.; Qi, Y.; Zhai, Z.; Lu, M.; Huang, N.; Zhang, B. Fluorine-modulated MXene-derived catalysts for multiphase sulfur conversion in lithium–sulfur battery. *Nano-Micro Lett.* **2024**, *16*, 266. [CrossRef]
50. Nanda, O.P.; Mukundan, G.; Deepak, M.S.; Badhulika, S. Synergistic performance of co-precipitated CoCuFe Prussian blue analogue and hydrothermally synthesized V_2C MXene in a solid-state asymmetric supercapacitor. *J. Energy Storage* **2024**, *96*, 112610. [CrossRef]
51. Guo, Y.; Jin, S.; Wang, L.; He, P.; Hu, Q.; Fan, L.-Z.; Zhou, A. Synthesis of two-dimensional carbide Mo_2CT_x MXene by hydrothermal etching with fluorides and its thermal stability. *Ceram. Int.* **2020**, *46*, 19550–19556. [CrossRef]
52. Huang, P.; Ying, H.; Zhang, S.; Zhang, Z.; Han, W.-Q. In situ fabrication of MXene/CuS hybrids with interfacial covalent bonding via Lewis acidic etching route for efficient sodium storage. *J. Mater. Chem. A* **2022**, *10*, 22135–22144. [CrossRef]
53. Liu, M.; Wang, L.; Zhang, L.; Zhao, Y.; Chen, K.; Li, Y.; Yang, X.; Zhao, L.; Sun, S.; Zhang, J. In-Situ Silica Xerogel Assisted Facile Synthesis of Fe-N-C Catalysts with Dense Fe-Nx Active Sites for Efficient Oxygen Reduction. *Small* **2022**, *18*, 2104934. [CrossRef]
54. Mahabari, K.; Mohili, R.D.; Patel, M.; Jadhav, A.H.; Lee, K.; Chaudhari, N.K. HF-free microwave-assisted synthesis of MXene as an electrocatalyst for hydrogen evolution in alkaline media. *Nanoscale Adv.* **2024**, *6*, 5388–5397. [CrossRef]
55. Li, T.; Yao, L.; Liu, Q.; Gu, J.; Luo, R.; Li, J.; Yan, X.; Wang, W.; Liu, P.; Chen, B. Fluorine-free synthesis of high-purity $Ti_3C_2T_x$ (T = OH, O) via alkali treatment. *Angew. Chem. Int. Ed.* **2018**, *57*, 6115–6119. [CrossRef]
56. Nandan, R.; Takamori, N.; Higashimine, K.; Badam, R.; Matsumi, N. Confronting the Issues Associated with the Practical Implementation of Zinc Blende-type SiC Anodes for Efficient and Reversible Storage of Lithium Ions. *ACS Appl. Energy Mater.* **2024**, *7*, 2088–2100. [CrossRef]
57. Yang, S.; Zhang, P.; Wang, F.; Ricciardulli, A.G.; Lohe, M.R.; Blom, P.W.; Feng, X. Fluoride-free synthesis of two-dimensional titanium carbide (MXene) using a binary aqueous system. *Angew. Chem. Int. Ed.* **2018**, *130*, 15717–15721. [CrossRef]
58. Pranada, E.; Ngozichukwu, B.; Yoo, R.; Johnson, D.; Barteau, M.A.; Abdel-Wahab, A.; Djire, A. Hydrogen Evolution and Oxygen Reduction on OH/F-Terminated Titanium Nitride MXene Reveal the Role of the Surface Termination Group in Electrocatalysis. *ACS Catal.* **2025**, *15*, 982–991. [CrossRef]
59. Hantanasirisakul, K.; Zhao, M.Q.; Urbankowski, P.; Halim, J.; Anasori, B.; Kota, S.; Ren, C.E.; Barsoum, M.W.; Gogotsi, Y. Fabrication of $Ti_3C_2T_x$ MXene transparent thin films with tunable optoelectronic properties. *Adv. Electron. Mater.* **2016**, *2*, 1600050. [CrossRef]
60. Li, M.; Lu, J.; Luo, K.; Li, Y.; Chang, K.; Chen, K.; Zhou, J.; Rosen, J.; Hultman, L.; Eklund, P. Element replacement approach by reaction with Lewis acidic molten salts to synthesize nanolaminated MAX phases and MXenes. *J. Am. Chem. Soc.* **2019**, *141*, 4730–4737. [CrossRef]
61. Defoy, E.; Baron, M.; Séné, A.; Ghoridi, A.; Thiaudière, D.; Célérier, S.; Chartier, P.; Brette, F.; Mauchamp, V.; Portehault, D. Galvanic Replacement and Etching of MAX-Related Phases in Molten Salts toward MXenes: An In Situ Study. *Chem. Mater.* **2023**, *35*, 8112–8121. [CrossRef]
62. Hussain, S.; Vikraman, D.; Mehran, M.T.; Hussain, M.; Nazir, G.; Patil, S.A.; Kim, H.-S.; Jung, J. Ultrasonically derived WSe_2 nanostructure embedded MXene hybrid composites for supercapacitors and hydrogen evolution reactions. *Renew. Energy* **2022**, *185*, 585–597. [CrossRef]

63. Vacík, J.; Horák, P.; Bakardjieva, S.; Bejsovec, V.; Ceccio, G.; Cannavo, A.; Torrisi, A.; Lavrentiev, V.; Klie, R. Ion sputtering for preparation of thin MAX and MXene phases. *Radiat. Eff. Defects Solids* **2020**, *175*, 177–189. [CrossRef]
64. Feng, K.; Xiao, B.; Wang, Y.; Yang, H.; Xiong, L.; Zhao, M.; Ma, J.; Li, B.; Guan, Y.; Ding, Y. Hexafluorozirconic acid-etched MXene for ammonium-ion capacitors. *J. Alloys Compd.* **2025**, *1010*, 177962. [CrossRef]
65. Huang, T.; Gao, B.; Zhao, S.; Zhang, H.; Li, X.; Luo, X.; Cao, M.; Zhang, C.; Luo, S.; Yue, Y. All-MXenes zinc ion hybrid micro-supercapacitor with wide voltage window based on V_2CT_x cathode and $Ti_3C_2T_x$ anode. *Nano Energy* **2023**, *111*, 108383. [CrossRef]
66. Zhao, J.; Wen, J.; Xiao, J.; Ma, X.; Gao, J.; Bai, L.; Gao, H.; Zhang, X.; Zhang, Z. Nb_2CT_x MXene: High capacity and ultra-long cycle capability for lithium-ion battery by regulation of functional groups. *J. Energy Chem.* **2021**, *53*, 387–395. [CrossRef]
67. Cai, Y.; Zhang, L.; Fang, R.; Wang, Y.; Wang, J. Maximized ion accessibility in the binder-free layer-by-layer MXene/CNT film prepared by the electrophoretic deposition for rapid hybrid capacitive deionization. *Sep. Purif. Technol.* **2022**, *292*, 121019. [CrossRef]
68. Pradhan, L.; Mohanty, B.; Padhy, G.; Trivedi, R.K.; Das, D.P.; Chakraborty, B.; Jena, B.K. Supercapacitor properties of partially oxidised-MXene quantum dots/graphene hybrids: Fabrication of flexible/wearable micro-supercapacitor devices. *Chem. Eng. J.* **2024**, *497*, 154587. [CrossRef]
69. Yang, L.; Cao, L.N.; Li, S.; Peng, P.; Qian, H.; Amaratunga, G.; Yang, F.; Wang, Z.L.; Wei, D. MOFs/MXene nano-hierarchical porous structures for efficient ion dynamics. *Nano Energy* **2024**, *129*, 110076. [CrossRef]
70. Xu, C.; Tong, L.; Chen, Y.; Bai, W.; Huang, Y.; Jiang, N.; Zhong, J.; Zhao, X.; Yang, L.; Yin, S. NiCo-LDH derived $NiCoS_2/TiVCT_x$ MXene/NC electrode materials with excellent low-temperature tolerance and reversible capacities for lithium-ion cells and lithium-sulfur batteries. *J. Alloys Compd.* **2025**, *1010*, 178133. [CrossRef]
71. Qu, C.; Li, S.; Zhang, Y.; Wang, T.; Wang, Q.; Chen, S. Surface modification of Ti_3C_2-MXene with polydopamine and amino silane for high performance nitrile butadiene rubber composites. *Tribol. Int.* **2021**, *163*, 107150. [CrossRef]
72. Guan, K.; Dong, L.; Xing, Y.; Li, X.; Luo, J.; Jia, Q.; Zhang, H.; Zhang, S.; Lei, W. Structure and surface modification of MXene for efficient Li/K-ion storage. *J. Energy Chem.* **2022**, *75*, 330–339. [CrossRef]
73. Kamila, S.; Chakraborty, B.; Basu, S.; Jena, B.K. Combined experimental and theoretical insights into energy storage applications of a VO_2 (D)–graphene hybrid. *J. Phys. Chem. C* **2019**, *123*, 24280–24288. [CrossRef]
74. Zhang, B.; Su, Y.; Chen, Y.; Qi, S.; Li, M.; Zou, W.; Jiang, G.; Zhang, W.; Gao, Y.; Pan, C. A Dielectric MXene-Induced Self-Built Electric Field in Polymer Electrolyte Triggering Fast Lithium-Ion Transport and High-Voltage Cycling Stability. *Angew. Chem. Int. Ed.* **2024**, *63*, e202403949. [CrossRef]
75. Yadav, S.; Kurra, N. Diffusion kinetics of ionic charge carriers across $Ti_3C_2T_x$ MXene-aqueous electrochemical interfaces. *Energy Storage Mater.* **2024**, *65*, 103094. [CrossRef]
76. Tang, H.; Li, W.; Pan, L.; Tu, K.; Du, F.; Qiu, T.; Yang, J.; Cullen, C.P.; McEvoy, N.; Zhang, C. A robust, freestanding MXene-sulfur conductive paper for long-lifetime Li–S batteries. *Adv. Funct. Mater.* **2019**, *29*, 1901907. [CrossRef]
77. Zhao, M.-Q.; Ren, C.E.; Ling, Z.; Lukatskaya, M.R.; Zhang, C.; Van Aken, K.L.; Barsoum, M.W.; Gogotsi, Y. Flexible MXene/carbon nanotube composite paper with high volumetric capacitance. *Adv. Mater.* **2014**, *27*, 339–345. [CrossRef]
78. Matthews, K.; Zhang, T.; Shuck, C.E.; VahidMohammadi, A.; Gogotsi, Y. Guidelines for synthesis and processing of chemically stable two-dimensional V_2CT_x MXene. *Chem. Mater.* **2021**, *34*, 499–509. [CrossRef]
79. Nasrallah, G.K.; Al-Asmakh, M.; Rasool, K.; Mahmoud, K.A. Ecotoxicological assessment of $Ti_3C_2T_x$ (MXene) using a zebrafish embryo model. *Environ. Sci. Nano* **2018**, *5*, 1002–1011. [CrossRef]
80. Xie, Y.; Naguib, M.; Mochalin, V.N.; Barsoum, M.W.; Gogotsi, Y.; Yu, X.; Nam, K.-W.; Yang, X.-Q.; Kolesnikov, A.I.; Kent, P.R. Role of surface structure on Li-ion energy storage capacity of two-dimensional transition-metal carbides. *J. Am. Chem. Soc.* **2014**, *136*, 6385–6394. [CrossRef]
81. Xu, S.; Dall'Agnese, Y.; Li, J.; Gogotsi, Y.; Han, W. Thermally Reduced Graphene/MXene Film for Enhanced Li-ion Storage. *Chem. Eur. J.* **2018**, *24*, 18556–18563. [CrossRef]
82. Zhu, J.; Zhu, S.; Cui, Z.; Li, Z.; Wu, S.; Xu, W.; Gao, Z.; Ba, T.; Liang, C.; Liang, Y. Dual Redox Reaction Sites for Pseudocapacitance Based on Ti and −P Functional Groups of $Ti_3C_2PBr_x$ MXene. *Angew. Chem. Int. Ed.* **2024**, *63*, e202403508. [CrossRef]
83. Shen, M.; Jiang, W.; Liang, K.; Zhao, S.; Tang, R.; Zhang, L.; Wang, J.Q. One-pot green process to synthesize MXene with controllable surface terminations using molten salts. *Angew. Chem. Int. Ed.* **2021**, *133*, 27219–27224. [CrossRef]
84. Kim, D.; Ko, T.Y.; Kim, H.; Lee, G.H.; Cho, S.; Koo, C.M. Nonpolar organic dispersion of 2D $Ti_3C_2T_x$ MXene flakes via simultaneous interfacial chemical grafting and phase transfer method. *ACS Nano* **2019**, *13*, 13818–13828. [CrossRef]
85. Sun, B.; Lu, Q.; Chen, K.; Zheng, W.; Liao, Z.; Lopatik, N.; Li, D.; Hantusch, M.; Zhou, S.; Wang, H.I. Redox-Active Metaphosphate-Like Terminals Enable High-Capacity MXene Anodes for Ultrafast Na-Ion Storage. *Adv. Mater.* **2022**, *34*, 2108682. [CrossRef]
86. Guo, Q.; Zhang, X.; Zhao, F.; Song, Q.; Su, G.; Tan, Y.; Tao, Q.; Zhou, T.; Yu, Y.; Zhou, Z. Protein-inspired self-healable Ti_3C_2 MXenes/rubber-based supramolecular elastomer for intelligent sensing. *ACS Nano* **2020**, *14*, 2788–2797. [CrossRef]

87. Liu, S.; Hu, F.; Shao, W.; Zhang, W.; Zhang, T.; Song, C.; Yao, M.; Huang, H.; Jian, X. A novel strategy of in situ trimerization of cyano groups between the $Ti_3C_2T_x$ (MXene) interlayers for high-energy and high-power sodium-ion capacitors. *Nano-Micro Lett.* **2020**, *12*, 135. [CrossRef]
88. Yoon, Y.; Tiwari, A.P.; Choi, M.; Novak, T.G.; Song, W.; Chang, H.; Zyung, T.; Lee, S.S.; Jeon, S.; An, K.S. Precious-metal-free electrocatalysts for activation of hydrogen evolution with nonmetallic electron donor: Chemical composition controllable phosphorous doped vanadium carbide MXene. *Adv. Funct. Mater.* **2019**, *29*, 1903443. [CrossRef]
89. Liu, Z.; Tian, Y.; Li, S.; Wang, L.; Han, B.; Cui, X.; Xu, Q. Revealing High-Rate and High Volumetric Pseudo-Intercalation Charge Storage from Boron-Vacancy Doped MXenes. *Adv. Funct. Mater.* **2023**, *33*, 2301994. [CrossRef]
90. Liang, Y.; Shen, H.; Li, J.; Zhao, H.; Xu, J.; Huang, H.; Xu, S.; Liang, X.; Zhou, W.; Guo, J. Tailoring surface terminals of $Ti_3C_2T_x$ MXene microgels via interlayer domain-confined polyphosphate ammonium for flexible supercapacitor applications. *Chem. Eng. J.* **2024**, *497*, 154775. [CrossRef]
91. Xu, J.; Peng, T.; Zhang, Q.; Zheng, H.; Yu, H.; Shi, S. Intercalation Effects on the Electrochemical Properties of $Ti_3C_2T_x$ MXene Nanosheets for High-Performance Supercapacitors. *ACS Appl. Nano Mater.* **2022**, *5*, 8794–8803. [CrossRef]
92. Guan, Y.; Jiang, S.; Ding, Y.; Xiao, B.; Pi, Y.; Wang, Z.; Cong, Y. Insight into the mechanism of nitrogen doping in MXenes with controllable surface chemistry. *Mater. Today Energy* **2024**, *44*, 101642. [CrossRef]
93. Ahmed, B.; Anjum, D.H.; Gogotsi, Y.; Alshareef, H.N. Atomic layer deposition of SnO_2 on MXene for Li-ion battery anodes. *Nano Energy* **2017**, *34*, 249–256. [CrossRef]
94. Wang, S.; Jin, D.; Bian, Y.; Wang, R.; Zhang, L. Electrostatically fabricated three-dimensional magnetite and MXene hierarchical architecture for advanced lithium-ion capacitors. *ACS Appl. Mater. Interfaces* **2020**, *12*, 9226–9235. [CrossRef]
95. Luo, Y.; Yang, C.; Tian, Y.; Tang, Y.; Yin, X.; Que, W. A long cycle life asymmetric supercapacitor based on advanced nickel-sulfide/titanium carbide (MXene) nanohybrid and MXene electrodes. *J. Power Sources* **2020**, *450*, 227694. [CrossRef]
96. Wang, X.; Li, H.; Li, H.; Lin, S.; Ding, W.; Zhu, X.; Sheng, Z.; Wang, H.; Zhu, X.; Sun, Y. 2D/2D 1T-MoS_2/Ti_3C_2 MXene heterostructure with excellent supercapacitor performance. *Adv. Funct. Mater.* **2020**, *30*, 0190302. [CrossRef]
97. Gao, Y.; Xue, P.; Ji, L.; Pan, X.; Chen, L.; Guo, W.; Tang, M.; Wang, C.; Wang, Z. Interfacial self-assembly of organics/MXene hybrid cathodes toward high-rate-performance sodium ion batteries. *ACS Appl. Mater. Interfaces* **2022**, *14*, 8036–8047. [CrossRef]
98. Meng, R.; Deng, Q.; Peng, C.; Chen, B.; Liao, K.; Li, L.; Yang, Z.; Yang, D.; Zheng, L.; Zhang, C. Two-dimensional organic-inorganic heterostructures of in situ-grown layered COF on Ti_3C_2 MXene nanosheets for lithium-sulfur batteries. *Nano Today* **2020**, *35*, 100991. [CrossRef]
99. Li, P.; Lv, H.; Li, Z.; Meng, X.; Lin, Z.; Wang, R.; Li, X. The electrostatic attraction and catalytic effect enabled by ionic–covalent organic nanosheets on MXene for separator modification of lithium–sulfur batteries. *Adv. Mater.* **2021**, *33*, 2007803. [CrossRef]

Disclaimer/Publisher's Note: The statements, opinions and data contained in all publications are solely those of the individual author(s) and contributor(s) and not of MDPI and/or the editor(s). MDPI and/or the editor(s) disclaim responsibility for any injury to people or property resulting from any ideas, methods, instructions or products referred to in the content.